AEDC-TR-70-290

cy 2

INSTABILITIES IN MHD ACCELERATORS

G. W. Garrison

ARO, Inc.

February 1971

PROPULSION WIND TUNNEL FACILITY
ARNOLD ENGINEERING DEVELOPMENT CENTER
AIR FORCE SYSTEMS COMMAND
ARNOLD AIR FORCE STATION, TENNESSEE

NOTICES

When U. S. Government drawings specifications, or other data are used for any purpose other than a definitely related Government procurement operation, the Government thereby incurs no responsibility nor any obligation whatsoever, and the fact that the Government may have formulated, furnished, or in any way supplied the said drawings, specifications, or other data, is not to be regarded by implication or otherwise, or in any manner licensing the holder or any other person or corporation, or conveying any rights or permission to manufacture, use, or sell any patented invention that may in any way be related thereto.

Qualified users may obtain copies of this report from the Defense Documentation Center.

References to named commercial products in this report are not to be considered in any sense as an endorsement of the product by the United States Air Force or the Government.

INSTABILITIES IN MHD ACCELERATORS

G. W. Garrison
ARO, Inc.

FOREWORD

The work reported herein was sponsored by Headquarters, Arnold Engineering Development Center (AEDC), Air Force Systems Command (AFSC), under Program Element 64719F.

The results of research presented were obtained by ARO, Inc. (a subsidiary of Sverdrup & Parcel and Associates, Inc.), contract operator of AEDC, AFSC, Arnold Air Force Station, Tennessee, under Contract F40600-71-C-0002. The investigation was conducted under ARO Project No. PW3805 from July 1967 to July 1968, and the manuscript was submitted for publication on September 22, 1970.

This technical report has been reviewed and is approved.

Thomas G. Horn
1/Lt, USAF
Facility Development
Division
Directorate of
Civil Engineering

Ernest F. Moore
Colonel, USAF
Director of
Civil Engineering

ABSTRACT

A linearized perturbation analysis is used to determine if instabilities can occur in MHD accelerators. When the electrical perturbations are assumed unaffected by the presence of conducting walls, the enthalpy wave has the largest growth rate. The growth rate depends upon the orientation of the current vector to the wave front and the location within the accelerator. When the electrical perturbations are influenced by the presence of the slanted conducting walls, the upstream-moving magneto-acoustic wave is amplified. When steady-state gradients are neglected, the growth rate changes only slightly in both cases. An elevated electron temperature increases the enthalpy wave growth rate in the absence of conducting walls, but has little effect when the conducting walls control the electrical perturbations. The linearized analysis indicates that instabilities can exist in MHD accelerators and the growth rate may be large in some cases.

CONTENTS

APPENDIXES

ILLUSTRATIONS

NOMENCLATURE

A	Area
A_1, A_2	Defined after Eq. (51) for one-dimensional perturbations
A_1, A_2, A_3	Defined in Eq. (86) for two-dimensional perturbations
a	Constant defined in Eq. (28)
a_0	Speed of sound
a_1, a_2, a_3	Defined in Eq. (I-9)
B	Magnetic flux density
B_i	Defined in Eq. (28)

B_1, B_2, B_3	Defined after Eq. (51) for one-dimensional case and in Eq. (86) for the two-dimensional case
b	Defined in Eq. (28)
b_1, b_2, b_3	Defined in Eq. (I-9) for one-dimensional case
b_1 through b_6	Defined in Eq. (86) for the two-dimensional case
C_1 through C_6	Coefficients in Dispersion Relation Eq. (52)
CA_1 through CA_4	Coefficients in Dispersion Relation Eq. (87)
CB_1 through CB_4	Coefficients in Dispersion Relation Eq. (87)
D	Defined in Eq. (62)
d	Channel height
E	Electric field
E_1, E_2, E_3	Defined in Eq. (86)
e	Perturbed electric field
F	Defined in Eq. (61)
F_x, F_y	Defined in Eq. (86)
G_1, G_2, G_3	Defined after Eq. (51)
H	Total enthalpy
h	Static enthalpy
I	Total current
J	Current density
j	Perturbed current density
k	Wave number or Boltzmann's constant
L	Characteristic length in x direction
M	Mach number
m	Particle mass
N, N_1, N_2	Defined after Eq. (51)
N_{ef}	Defined in Eq. (86)
n	Particle number density
P	Defined in Eq. (86)
p	Pressure

q_1	Defined after Eq. (I-4) for Case I and after Eq. (56) for Case II
q_2 through q_4	Defined after Eq. (45) for Case I
R	Gas constant
R_σ	Defined in Eq. (60)
S_m	Seed fraction by mole
T	Temperature
V	Perturbed electric potential
V_i	Seed ionization energy
u, v	Velocity components in x, y directions, respectively
w	Enthalpy exponent defined after Eq. (66)
x, y, z	Cartesian coordinates
α	Ionization fraction
β	Hall coefficient
β_{ef}	Reduced Hall coefficient = $\beta_o/(1 + \beta_o^2)$
γ	Gas specific heat ratio
γ_1 through γ_3	Defined after Eq. (46) for Case I and after Eq. (56) for Case II
δ_s	Energy loss factor of electrons interacting with species s
δ_{eff}	Effective energy loss factor of the gas
ϵ	Angle between current vector and wave front
θ	Wall slant angle
λ	Disturbance wavelength
μ_1, μ_2, μ_3	Defined after Eq. (I-6)
ν	Collision frequency
ξ_1, ξ_2, ξ_3	Defined after Eq. (I-6)
ρ	Density
σ	Electrical conductivity
σ_{ef}	Reduced electrical conductivity = $\sigma_o/(1 + \beta_o^2)$

τ	Average time between collisions
Φ	Tangent of wall slant angle
$\phi_1, \phi_2, \phi_3, \phi_4$	Defined after Eq. (I-4)
ϕ	Perturbed velocity potential function
ψ	Perturbed current density potential function
ω	Complex disturbance frequency = $\omega_1 + i\omega_2$

SUBSCRIPTS

1	Perturbation quantity
e	Electrons
f	Final value
i	Initial value
K	Potassium
s	Species other than electrons
x	Component in x direction
y	Component in y direction
o	Steady-state quantity

SECTION I
INTRODUCTION

The prediction of magnetohydrodynamic (MHD) accelerator performance requires an understanding of the basic flow phenomena and parameters which affect their operation. The presence of any disturbance which is significantly amplified can greatly affect the operation of these devices. Previous investigations considering the growth of disturbances in MHD generators have indicated that the growth can be significant in some cases. The purpose of this investigation is to determine if disturbances can grow in MHD accelerators resulting in an instability which can affect the performance of the device.

There are three types of disturbances which may result in an instability in the high density, highly resistive plasmas utilized in MHD accelerators. The "electrothermal" (ionization) instability, first postulated by Kerrebrock (Ref. 1), is the result of preferential heating of the electron gas with the heavy gas species unaffected. One necessary criterion for the amplification of these "electrothermal waves" is that the electron gas be loosely coupled to the heavy gas (Refs. 1 and 2). The coupling between the electrons and heavy species in MHD accelerators using diatomic gases is quite strong and, hence, the electrothermal disturbance is not expected to lead to instabilities.

The enthalpy wave is similar to the electrothermal wave but involves localized heating of the entire gas. A localized "hot spot" in the gas is heated further because of the local increase in conductivity and hence increased joule heating. The growth rate of an enthalpy wave will be much less than that of an electrothermal wave because of the larger specific heat of the gas. However, in contrast to the electrothermal wave, the enthalpy wave can exist in the MHD accelerators of interest.

The amplification of the magneto-acoustic disturbance is directly dependent on the fluctuations of the thermodynamic properties of the gas (Ref. 3) and has a large growth when the electrons and heavy species are strongly coupled (Ref. 2). This type of instability, first postulated by Velikhov (Ref. 4), depends directly on the Hall effect in the first approximation. A simple physical model of this disturbance can be constructed in the following manner (Refs. 2 and 3). Consider the case of the total steady-state current in the y direction and the magnetic field, B, in the z direction as shown in Fig. 1.

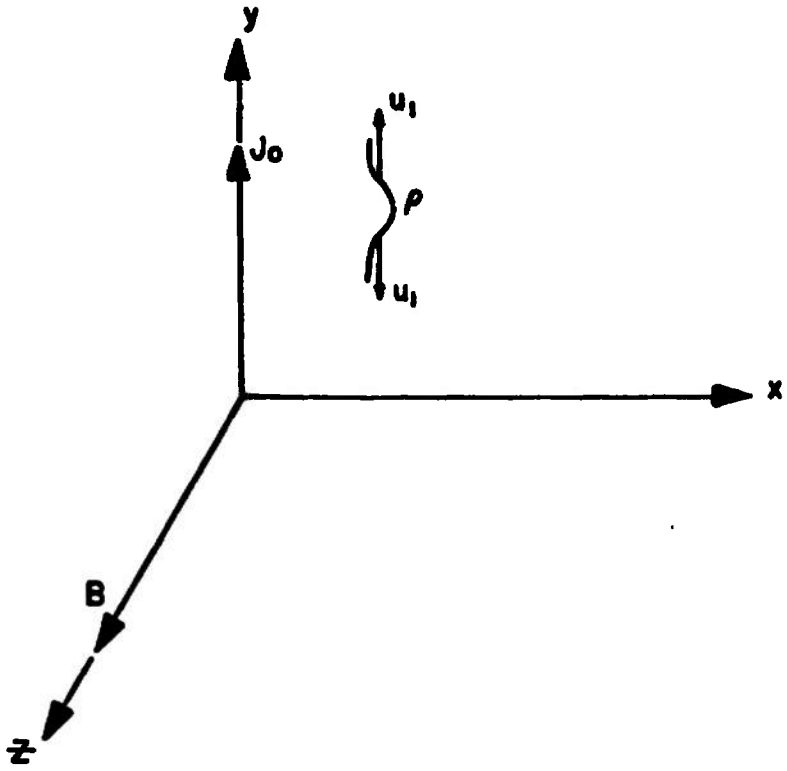

Fig. 1 Simple Model for a Magneto-Acoustic Disturbance

In the presence of a positive density perturbation propagating parallel or antiparallel to $\vec{J}_o$, an induced current, $\sigma_o(\vec{u} \times \vec{B})$, will flow. The resulting force $\sigma_o(\vec{u} \times \vec{B}) \times \vec{B}$ will always oppose the propagation and, hence, damp the disturbance. However, the positive density perturbation results in a local decrease in the Hall parameter, β. The decrease in β means that the x component of the electric field has too large a value for the local conditions and therefore a perturbation current, J_h, will flow in the positive x direction. This current interacting with the magnetic field will amplify the disturbance moving antiparallel to J_o and attenuate the disturbance moving parallel to J_o. The condition for instability, given initially by Velikhov (Ref. 4), is that $J_h > \sigma_o$ u B when there are fluctuations only in β.

Detailed analyses (Ref. 3), including perturbations in conductivity, pressure, density, velocity, and Hall parameter, indicate that, depending on the frequency, the initial steady state of the plasma, and the orientation of the wave vector, waves can be amplified at a rate significantly higher than that indicated by Velikhov. The analyses (Refs. 5, 6, and 7) of the transverse and longitudinal waves in a generator operating in the Faraday mode indicate that the growth rate is small and the instability can be controlled by external circuitry. However, the growth of axial waves in a Hall-type generator was found to be significant (Ref. 8). The growth rates of the waves have, in general, been found to increase with decreasing pressure (Ref. 9) or increasing specific heat ratio (Refs. 8 and 10). The results of these investigations indicate that instabilities can exist in MHD generators.

On the basis of the substantial evidence that instabilities can exist in MHD generators, there is reason to believe that instabilities can also exist in accelerators. The investigation of magneto-acoustic and enthalpy disturbances in MHD accelerators is the primary concern of this report. The method of analysis will be to assume that the steady-state flow is given by the solution of the usual quasi-one-dimensional gas dynamic equations with MHD terms. The flow is subjected to a small perturbation, and the behavior of this distrubance is investigated using a linearized analysis.

SECTION II
MATHEMATICAL MODEL

The equations describing the flow of an inviscid, nonheat-conducting, slightly ionized gas in the presence of electric and magnetic fields can be written in the form (Ref. 11):

$$\text{Mass:} \qquad \frac{\partial \rho}{\partial t} + \nabla \cdot \rho \vec{v} = 0 \tag{1}$$

$$\text{Momentum:} \qquad \rho \frac{\partial \vec{v}}{\partial t} + \rho \vec{v} \cdot \nabla \vec{v} = - \nabla p + \vec{J} \times \vec{B} \tag{2}$$

$$\text{Energy:} \qquad \rho \frac{\partial H}{\partial t} + \rho \vec{v} \cdot \nabla H - \frac{\partial p}{\partial t} = \vec{J} \cdot \vec{E} \tag{3}$$

where ρ is the density, $\vec{v}$ is the velocity, p is the pressure, $\vec{J}$ is the total current density, $\vec{B}$ is the applied magnetic field, $\vec{E}$ is the stationary electric field, and H is the total enthalpy given by

$$H = h + \frac{\vec{v} \cdot \vec{v}}{2} \tag{4}$$

where h is the static enthalpy. The electric current density is given by Ohm's law, including the Hall effect, as

$$\vec{J} = \frac{\sigma}{1 + \beta^2} \left\{ \vec{E} + \vec{v} \times \vec{B} - \frac{\beta}{B} \left[\vec{E} \times \vec{B} + (\vec{v} \times \vec{B}) \times \vec{B} \right] \right\} \tag{5}$$

where σ is the electrical conductivity and β is the Hall coefficient.

2.1 STEADY-STATE SOLUTION

The steady accelerator flow is assumed to be given by the quasi-one-dimensional gas dynamic equations including MHD effects. Using the quasi-one-dimensional approximations in Eqs. (1), (2), and (3), the equations for the steady state are

$$\rho_o u_o A = \dot{m} \tag{6}$$

$$\rho_o u_o \frac{du_o}{dx} = - \frac{dp_o}{dx} + J_y B \tag{7}$$

$$\rho_o u_o \frac{dH_o}{dx} = J_x E_x + J_y E_y \tag{8}$$

where u is the velocity in the x direction and $\dot{m}$ is the mass flow rate.

An MHD accelerator channel having slanted electrodes and connected in the two-terminal mode (Fig. 2 and Ref. 12) is to be considered.

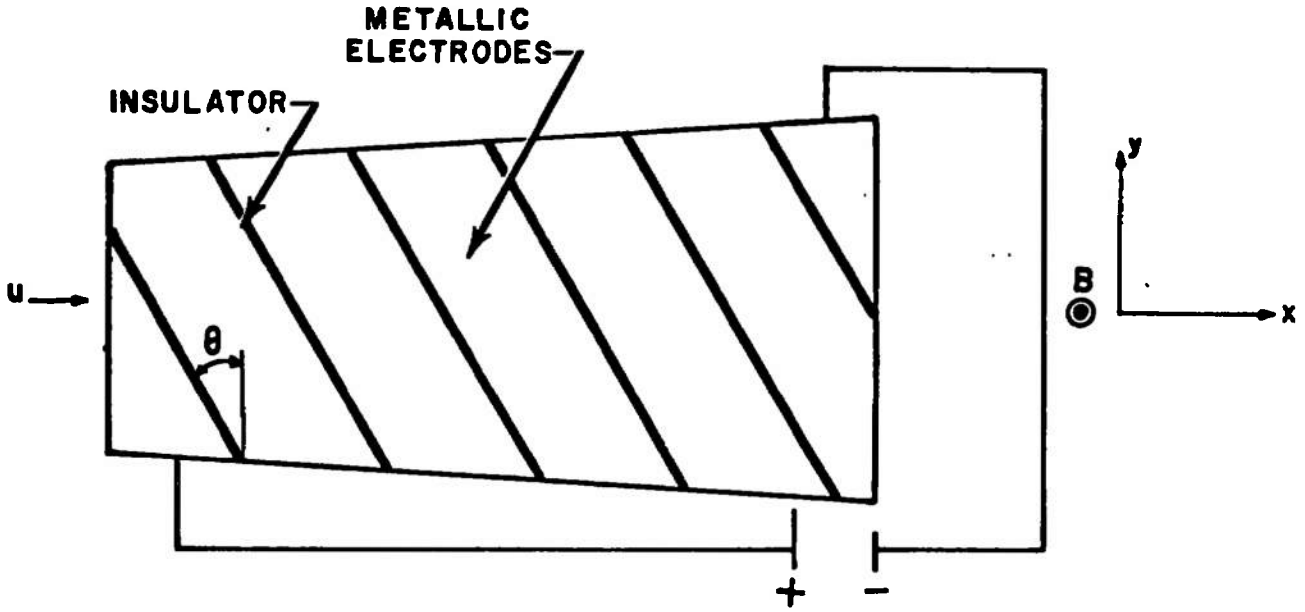

Fig. 2 Slant-Wall Accelerator Connected for Two-Terminal Operation

For this case the generalized Ohm's law can be written in component form as

$$J_x = \frac{\sigma_o}{1 + \beta_o^2}\left\{E_x - \beta_o(E_y - u_o B)\right\} \tag{9}$$

$$J_y = \frac{\sigma_o}{1 + \beta_o^2}\left\{E_y - u_o B + \beta_o E_x\right\} \tag{10}$$

Two additional relations exist between the electrical parameters when operating a slant-wall accelerator in the two-terminal mode; that is

$$E_y = \Phi_o E_x \tag{11}$$

$$I = A(J_x + \Phi_o J_y) \tag{12}$$

where $\Phi_o = \tan\theta$, I is the total current supplied to the channel, A is the channel cross-sectional area, and θ is the channel slant-wall angle. The voltage drop at the electrode surface has been neglected in this analysis. Using Eqs. (11) and (12) in Eqs. (9) and (10) results in the following expressions for J_x, J_y, and E_x:

$$J_x = \frac{I}{A}\left(\frac{1 - \beta_o\Phi_o}{1 + \Phi_o^2}\right) + \frac{\Phi_o}{1 + \Phi_o^2}\,\sigma_o u_o B \tag{13}$$

$$J_y = \frac{I}{A}\left(\frac{\Phi_o + \beta_o}{1 + \Phi_o^2}\right) - \frac{\sigma_o u_o B}{1 + \Phi_o^2} \tag{14}$$

$$E_x = \frac{(I/A)(1 + \beta_o^2) - \sigma_o u_o B(\beta_o - \Phi_o)}{\sigma_o(1 + \Phi_o^2)} \tag{15}$$

Solutions to Eqs. (6) through (8) and (13) through (15) for given values of I, A, and B, which may vary with x, and with specified initial conditions have been obtained. The solution shown in Fig. 3 for potassium-seeded air in chemical equilibrium was used for the stability analysis presented here. Other operating conditions were considered, but the general criteria for instability did not change from the results obtained utilizing this solution.

2.2 PERTURBATION EQUATIONS

The response of the plasma to small disturbances will be investigated using a small perturbation analysis. The externally applied magnetic field is assumed constant with respect to the perturbation and induced magnetic fields are neglected since the magnetic Reynolds number is small. The velocity, thermodynamic, and electrical parameters are assumed to undergo a small perturbation; that is

$$\begin{aligned}
\vec{v} &= \vec{v}_o + \vec{v}_1 = \hat{i}(u_o + u_1) + \hat{j}(v_1) \\
\vec{J} &= \vec{J}_o + \vec{j} = \hat{i}(J_x + j_x) + \hat{j}(J_y + j_y) \\
\vec{E} &= \vec{E}_o + \vec{e} = \hat{i}(E_x + e_x) + \hat{j}(E_y + e_y)
\end{aligned} \tag{16}$$

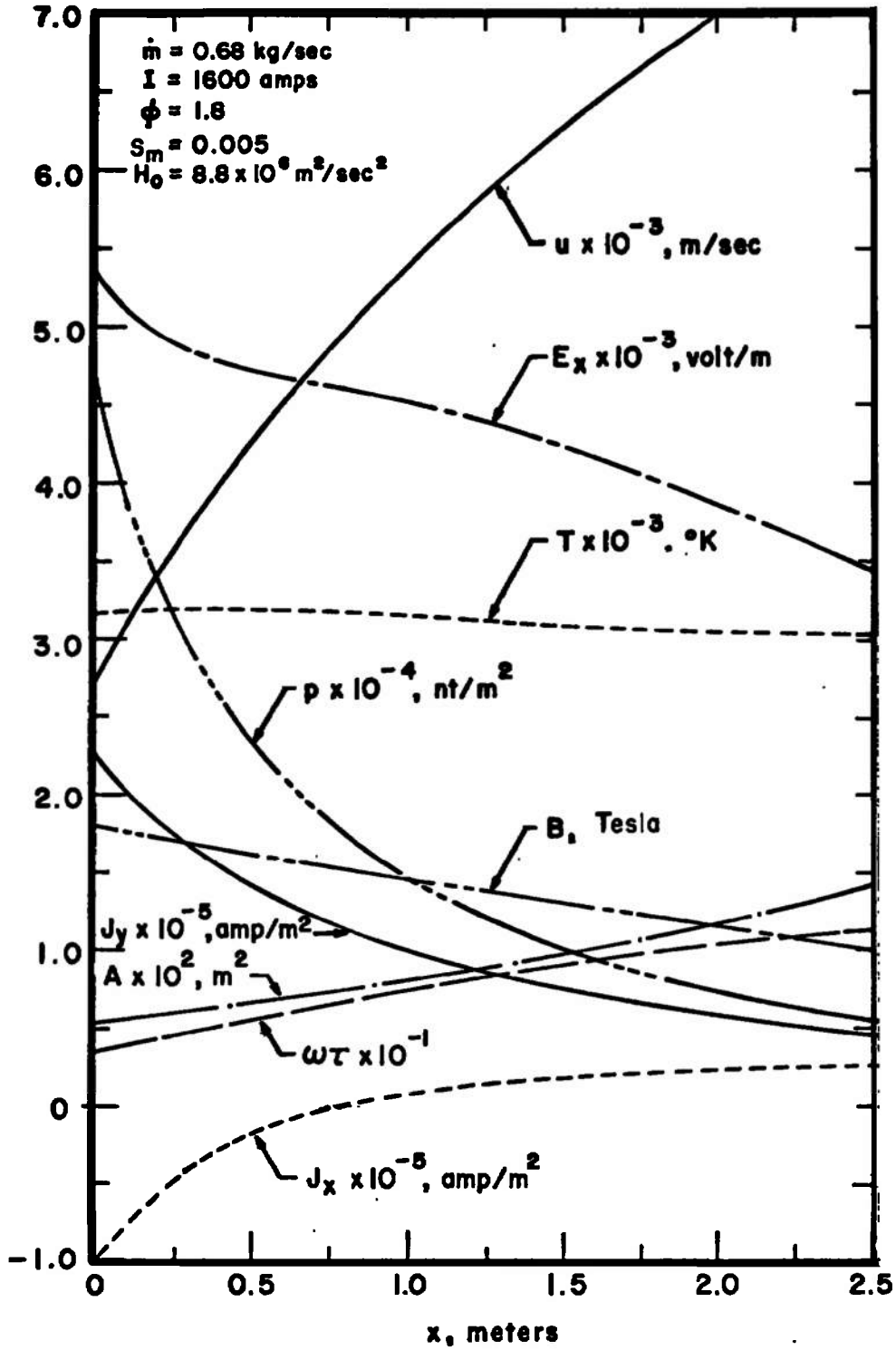

Fig. 3 Steady-State Solution for a Slant-Wall Accelerator

Substituting the perturbed variables into Eqs. (1), (2), (3), (9), and (10) and neglecting higher-order terms results in the following perturbation equations:

Continuity:

$$\frac{\partial \rho_1}{\partial t} + u_o \frac{\partial \rho_1}{\partial x} + \rho_1 \frac{\partial u_o}{\partial x} + u_1 \frac{\partial \rho_o}{\partial x} + \rho_o \left(\frac{\partial u_1}{\partial x} + \frac{\partial v_1}{\partial y}\right) = 0 \quad (17)$$

x-Momentum:

$$\rho_o \frac{\partial u_1}{\partial t} + \rho_o u_o \frac{\partial u_1}{\partial x} + \rho_o u_o \frac{\partial u_o}{\partial x} \left(\frac{\rho_1}{\rho_o} + \frac{u_1}{u_o}\right) = - \frac{\partial p_1}{\partial x} + j_y B \quad (18)$$

y-Momentum:

$$\rho_o \frac{\partial v_1}{\partial t} + \rho_o u_o \frac{\partial v_1}{\partial x} = - \frac{\partial p_1}{\partial y} - j_x B \quad (19)$$

Energy:

$$\rho_o \frac{\partial H_1}{\partial t} + \rho_o u_o \frac{\partial H_1}{\partial x} + \rho_o u_o \frac{\partial H_o}{\partial x} \left(\frac{u_1}{u_o} + \frac{\rho_1}{\rho_o}\right) - \frac{\partial p_1}{\partial t} = \vec{E}_o \cdot \vec{j} + \vec{e} \cdot \vec{J}_o \quad (20)$$

Ohm's Law:

$$j_x = \sigma_{ef} \left\{ e_x + v_1 B - \beta_o (e_y - u_1 B) - \beta_1 (E_y - u_o B) \right\} + J_x \left\{ \frac{\sigma_1}{\sigma_o} - 2 \beta_{ef} \beta_1 \right\} \quad (21)$$

$$j_y = \sigma_{ef} \left\{ e_y - u_1 B + \beta_o (e_x + v_1 B) + \beta_1 E_x \right\} + J_y \left\{ \frac{\sigma_1}{\sigma_o} - 2 \beta_{ef} \beta_1 \right\} \quad (22)$$

where

$$\sigma_{ef} = \frac{\sigma_o}{1 + \beta_o^2} \qquad \beta_{ef} = \frac{\beta_o}{1 + \beta_o^2}$$

This general form of the perturbed Ohm's law will be utilized in later sections when special forms of the perturbed equations are considered.

The four partial differential equations (Eqs. (17) through (20)) and the two algebraic equations (Eqs. (21) and (22)) contain the twelve unknown perturbation quantities p_1, ρ_1, u_1, v_1, σ_1, H_1, β_1, j_y, j_x, e_x, and e_y. The first four of these are taken as the primary dependent variables along with j_x and j_y. In order to obtain a closed set of equations, additional relations are needed between these and the remaining perturbation quantities.

The perturbed state properties are assumed to follow an ideal gas behavior, both calorically and thermally. Based on this assumption, the perturbed enthalpy, pressure, density, and temperature can be related in the following manner:

$$H_1 = \frac{\gamma}{\gamma - 1} \frac{p_o}{\rho_o} \left(\frac{p_1}{p_o} - \frac{\rho_1}{\rho_o} \right) + u_o u_1 \tag{23}$$

and

$$\frac{T_1}{T_o} = \frac{p_1}{p_o} - \frac{\rho_1}{\rho_o} \tag{24}$$

where γ is the specific heat ratio which is not perturbed. When making calculations, the specific heat ratio was evaluated at the thermodynamic conditions given by the steady-state solution.

The electrical conductivity, σ_1, and Hall coefficient, β_1, will now be related to the thermodynamic parameters, T_1, ρ_1, p_1, T_{e1}, and n_{e1}. The Hall coefficient is defined as

$$\beta = \omega\tau = \frac{eB}{m_e} \tau \tag{25}$$

where e is the electronic charge, m_e is the electron mass, and τ is the mean free-time between collision of electrons with other particles. In like manner the electrical conductivity can be written as

$$\sigma = \frac{n_e e^2}{m_e} \tau \tag{26}$$

where n_e is the electron number density. Eliminating τ between Eqs. (25) and (26) and perturbing, the following relation between σ_1, β_1, and n_{e_1} results

$$\frac{\beta_1}{\beta_o} = \frac{\sigma_1}{\sigma_o} - \frac{n_{e_1}}{n_{e_o}} \tag{27}$$

Since the exact expression for the electrical conductivity is more complex than is necessary for this analysis, a simpler form is used

$$\sigma \sim \frac{S_m{}^a}{p^{1/2}} T_e{}^b \, e^{-\frac{B_i}{T_e}} \tag{28}$$

where S_m is the seed fraction on a mole basis and T_e is the electron temperature. The constants a, b, and B_i can be picked from curve fits of the electrical conductivity for the range of seed fraction and temperature of interest. The values used in this analysis were a = 0.27, b = 0.75, and B_i = 22,180°K. These correspond to a seeded air plasma dominated by electron-neutral collisions. The perturbed conductivity can now be written as

$$\frac{\sigma_1}{\sigma_o} = a \frac{\rho_1}{\rho_o} - \frac{1}{2} \frac{p_1}{p_o} + \left(b + \frac{B_i}{T_{e_o}}\right) \frac{T_{e_1}}{T_{e_o}} \tag{29}$$

where it has been assumed that the perturbation of the seed fraction follows the gas density; i.e., $(S_{m_1}/S_{m_o}) = (\rho_1/\rho_o)$.

The electron number density can be obtained from the Saha equation evaluated at the electron temperature

$$\frac{n_e{}^2}{n_K - n_e} = \left[\frac{2\pi \, m_e \, k}{h^2}\right]^{3/2} T_e{}^{3/2} \, e^{-\frac{e \, V_i}{k \, T_e}} \tag{30}$$

where n_K is the number density of seed nuclei present (seed rate), k is Boltzmann's constant, h is Plank's constant, and V_i is the ionization energy of the seed. For disturbances of reasonably low frequency (up to about a megahertz), the electrons are assumed to remain in local Saha equilibrium and from Eq. (30) the perturbed electron number density can be expressed as

$$\frac{n_{e_1}}{n_{e_o}} = \frac{1}{2 \, S_{m_o} - \alpha_o} \left\{(S_{m_o} - \alpha_o)\left(\frac{3}{2} + \frac{e \, V_i}{k \, T_{e_o}}\right) \frac{T_{e_1}}{T_{e_o}} + S_{m_o} \frac{\rho_1}{\rho_o}\right\} \tag{31}$$

where α_{o_1} is the steady-state ionization fraction. Using Eqs. (29) and (31) in Eq. (27) results in the following expression for the perturbed Hall coefficient

$$\frac{\beta_1}{\beta_o} = -\frac{1}{2}\frac{p_1}{p_o} + \left(a - \frac{S_{m_o}}{2S_{m_o} - \alpha_o}\right)\frac{\rho_1}{\rho_o} + \frac{T_{e_1}}{T_{e_o}}\left\{b + \frac{B_i}{T_{e_o}} - \left(\frac{S_{m_o} - \alpha_o}{2S_{m_o} - \alpha_o}\right)\left(\frac{3}{2} + \frac{e V_i}{k T_{e_o}}\right)\right\} \tag{32}$$

The only variables remaining unspecified in Eqs. (29) and (32) are the steady-state and perturbed electron temperatures (T_{e_o} and T_{e_1}). Since the purpose of this analysis is to investigate the effects of various parameters on the stability of disturbances in the flow, the steady-state electron temperature will be specified by fixing the quantity ($T_{e_o} - T_o$). When the electrons are in thermal equilibrium ($T_o = T_{e_o}$) Eq. (24) can be used for the perturbed electron temperature. When thermal nonequilibrium exists, the perturbed electron temperature is determined from the electron energy equation. Simplifying the electron energy equation by equating the energy input to the electron gas with the energy loss attributable to collisions of electrons with other species, we have

$$\frac{J^2}{\sigma} = \frac{3}{2} k n_e m_e \sum_{s \neq e}\left(\frac{\delta_s \nu_{es}}{m_s}\right)(T_e - T) \tag{33}$$

where δ_s is the energy loss factor for electron collisions with species s and ν_{es} is the collision frequency of the electrons with species s.

An effective electron energy loss factor can be defined as

$$\delta_{eff} = \frac{\sum_{s \neq e} \delta_s \frac{m_e}{m_s} \nu_{es}}{\sum_{s \neq e} \nu_{es}} = \tau \sum_{s \neq e} \delta_s \frac{m_s}{m_e} \nu_{es}$$

Then using Eq. (26), Eq. (33) is written as

$$J^2 = \frac{3}{2} k \frac{n_e^2 e^2}{m_e} \delta_{eff}(T_e - T) \tag{34}$$

Assuming δ_{eff} is constant and using Eqs. (29) and (31) the perturbed equation is

$$\frac{2\,J_y j_y + 2\,J_x j_x}{J_x^2 + J_y^2} = \left(2\,\mu_1 + \frac{T_{e_o}}{T_{e_o} - T_o}\right)\frac{T_{e_1}}{T_{e_o}} - \frac{T_o}{T_{e_o} - T_o}\frac{p_1}{p_o} + \left(\frac{2\,S_{m_o}}{2\,S_{m_o} - \alpha_o} + \frac{T_o}{T_{e_o} - T_o}\right)\frac{\rho_1}{\rho_o} \tag{35}$$

where

$$\mu_1 = \left(\frac{S_{m_o} - \alpha_o}{2\,S_{m_o} - \alpha_o}\right)\left(\frac{3}{2} + \frac{eV_i}{kT_{e_o}}\right)$$

Equation (35) is an implicit expression for T_{e_1}/T_{e_o} since j_y and j_x depend on T_{e_1}/T_{e_o} through σ_1/σ_o and β_1/β_o. An explicit expression will be obtained for the various cases considered in the following sections.

The number of unknowns has been reduced to six: ρ_1, p_1, u_1, v_1, e_y, and e_x. Additional conditions for the electrical properties must be obtained to form a closed set of equations. In addition to Eqs. (17), (18), (19), and (20), the perturbation quantities must also satisfy, in some sense, the following relations

$$\nabla \cdot \vec{j} = \frac{\partial j_x}{\partial x} + \frac{\partial j_y}{\partial y} = 0 \tag{36}$$

$$\nabla \times \vec{e} = 0 \quad \text{or} \quad \frac{\partial e_y}{\partial x} = \frac{\partial e_x}{\partial y} \tag{37}$$

$$\frac{e_y}{E_y} = \frac{\Phi_1}{\Phi_o} + \frac{e_x}{E_x} \tag{38}$$

$$\frac{I_1}{A} = j_x + \Phi_o j_y + \Phi_1 J_y \tag{39}$$

where Φ_1 and I_1 are the perturbed tangent of the equipotential slant angle and total current, respectively. Although the equipotential surface may remain fixed at the walls because of the presence of the slanted electrodes, the local equipotential surface within the gas may change if E_x and E_y are not perturbed in such a manner as to remain in the same ratio ($e_y \neq \Phi_o e_x$).

In order to investigate the stability of the slant-wall MHD accelerator to small disturbances, three essentially different cases will be considered. In two of the cases, it is assumed that the disturbances are planar waves moving in the axial direction. The third case considers disturbances which can be a function of the transverse coordinate as well as the axial coordinate.

SECTION III
ONE-DIMENSIONAL PERTURBATIONS

The perturbations are assumed to be in the form of one-dimensional plane traveling waves moving along the x axis and are dependent only on the x coordinate. The time and spatial derivatives of the small disturbances are reduced by Fourier analyzing in time and space by assuming the waves are of the form

$$e^{i(kx-\omega t)} \tag{40}$$

where k is the wave number which is assumed to be real and $\omega = \omega_1 + i\omega_2$ is the complex frequency. The wavelength $\lambda = 2\pi/k$ and the frequency ω are taken to be independent of x. This requires that the wavelength must be short compared to the distance over which the steady-state parameters vary appreciably.

The stability of the disturbance can also be investigated by assuming k complex and ω real. This is equivalent to investigating the growth of the disturbance as it propagates in the device at a given frequency, in contrast to investigating the growth in time for a given wavelength (k). It was shown in Ref. 10 that a wave must grow in time and space simultaneously if the instability is indicated in either case. Equivalent results were found in the cases considered here using either approach. In the following, k is assumed real and ω is assumed complex.

When the perturbations are independent of y, Eqs. (36) and (40) reduce to

$$\frac{\partial j_x}{\partial x} = 0 \text{ or } j_x = 0$$

$$\frac{\partial e_y}{\partial x} = 0 \text{ or } e_y = 0 \tag{41}$$

This implies then that the perturbation current flows transverse to the wave front, and the electric field is perturbed normal to the wave front. The plasma is infinite compared to the scale of the disturbance, and Eq. (41) represents the additional relationship needed to complete the solution. Equations (38) and (39) may be used to determine the local perturbations Φ_1 and I_1 but are not necessary for completing the analysis. For the condition in Eq. (41), Eqs. (38) and (39) may be expressed as

$$\frac{\Phi_1}{\Phi_0} = -\frac{e_x}{E_x}$$

$$\frac{I_1}{A} = \Phi_0 j_y + \Phi_1 J_y \tag{42}$$

i. e., both the equipotential slant angle and total current are changed from their steady-state value.

If it is assumed that the equipotential angle θ is not perturbed and that the total current is constant, then from Eqs. (38) and (39) it follows that

$$e_y = \Phi_0 e_x \tag{43}$$

$$j_x = -\Phi_0 j_y \tag{44}$$

This implies that the plasma is finite and the accelerator conducting walls have a considerable influence on the disturbance. These relations together with the assumed form of the wave, Eq. (40), are incompatible with Eqs. (36) and (37) which cannot be satisfied exactly. This is analogous to the steady-state quasi-one-dimensional solution where the

equations are not satisfied in an exact sense. The essential requirement is that J and E are slowly varying functions of x so that the one-dimensional equations are approximately satisfied. The same requirement for the perturbation quantities e_y and j_x approximately satisfies the perturbation equations. From Eqs. (37) and (40) it can be seen that

$$\frac{\partial e_y}{\partial x} = i\ k\ e_y \approx 0$$

implies that the disturbance must necessarily have a long wavelength ($k < 1$) and/or the slant angle θ is small so that $e_y = \Phi_o\ e_x$ is small.

The requirement that the disturbance have a relatively long wavelength contradicts the earlier requirement that the wavelength should be short compared to the x variation of the various steady-state parameters (u_o, p_o, ρ_o). It can be seen that these conditions cannot always be satisfied simultaneously and, hence, all of the equations are not satisfied exactly. However, the analysis should indicate what effect boundaries have on disturbance growth. Equations (43) and (44) represent the additional relationships needed to complete the solution.

Hence, two different cases can be considered: (1) the plasma is infinite compared to the scale of the disturbance, and Eqs. (38) and (39) are redundant; (2) the plasma is finite compared to the scale of disturbance, and the boundary conditions of constant current and constant equipotential angle must be satisfied.

3.1 DISTURBANCE IN AN INFINITE PLASMA (CASE I)

Since the perturbation velocity field is approximately irrotational ($\nabla \times \vec{v} = 0$), Ref. 8, the transverse perturbation velocity, v_1, is approximately zero. Using this fact and the results from Eq. (41) in Eq. (19) shows that the perturbation pressure also depends only on the x coordinate. The y-momentum equation has thus been approximately satisfied. The current density, j_y, joule heating, $j_y E_y + J_x e_x$, conductivity, σ_1, Hall coefficient, β_1, and electron temperature can now be expressed in terms of p_1, ρ_1, and u_1 which are taken to be the independent variables.

Using Eqs. (21) and (22), noting $j_x = e_y = 0$, and eliminating e_x yields the following expression for j_y

$$j_y = - q_2 \frac{u_1}{u_o} + q_3 \frac{\sigma_1}{\sigma_o} + q_4 \frac{\beta_1}{\beta_o} \qquad (45)$$

where

$$q_2 = \sigma_o u_o B$$

$$q_3 = J_y - \beta_o J_x$$

$$q_4 = \beta_o J_x$$

The joule heating, $J_x e_x + j_y E_y$, can be expressed as follows

$$J_x e_x + j_y E_y = \gamma_1 \frac{\sigma_1}{\sigma_o} + \gamma_2 \frac{\beta_1}{\beta_o} + \gamma_3 \frac{u_1}{u_o} \tag{46}$$

where

$$\gamma_1 = (J_y - \beta_o J_x) E_y - J_x^2/\sigma_{ef}$$

$$\gamma_2 = \frac{\beta_o J_x}{\sigma_o} (J_y + \beta_o J_x + \sigma_o E_y)$$

$$\gamma_3 = - u_o B(\sigma_o E_y + \beta_o J_x)$$

The perturbed quantities σ_1/σ_o and β_1/β_o can now be related to the variables u_1, p_1, and ρ_1 by using the expressions developed in the preceding sections. Arriving at the final expressions involves some tedious algebra, and their development can be found in Appendix I along with the final coefficients. Using the coefficients from Appendix I, j_y and the joule heating can be expressed as

$$j_y = a_1 \frac{\rho_1}{\rho_o} + a_2 \frac{p_1}{p_o} + a_3 \frac{u_1}{u_o} \tag{47}$$

$$j_y E_y + e_x J_x = b_1 \frac{\rho_1}{\rho_o} + b_2 \frac{p_1}{p_o} + b_3 \frac{u_1}{u_o} \tag{48}$$

The perturbed Eqs. (17), (18), and (20) can now be reduced to three homogeneous algebraic equations in the unknowns u_1, ρ_1, and p_1. Substituting Eqs. (47) and (48) into Eqs. (17), (18), and (20) and using Eqs. (23) and (40), the algebraic equations can be written in nondimensional form as

$$\frac{\rho_1}{\rho_o}\left(\bar{\omega} - \bar{k} + iG_1\right) + \frac{u_1}{u_o}\left(-\bar{k} + iG_1\right) = 0 \tag{49}$$

$$\frac{\rho_1}{\rho_o} A_1 + \frac{u_1}{u_o}\left[A_2 + i\left(-\bar{\omega} + \bar{k}\right)\right] + \frac{p_1}{p_o}\left(-N_2 + i\frac{\bar{k}}{\gamma M^2}\right) = 0 \tag{50}$$

$$\frac{\rho_1}{\rho_o}\left[B_1 + i\left(\bar{\omega} - \bar{k}\right)\right] + \frac{u_1}{u_o}\left[B_2 + i\left(\bar{\omega} - \bar{k}\right)(\gamma - 1)M^2\right] + \frac{p_1}{p_o}\left[B_3 + i\left(-\frac{\bar{\omega}}{\gamma} + \bar{k}\right)\right] = 0 \tag{51}$$

where

$$G_1 = \frac{L}{\rho_o}\frac{d\rho_o}{dx}$$

$$G_2 = \frac{L}{u_o}\frac{du_o}{dx}$$

$$G_3 = \frac{L}{p_o}\frac{dp_o}{dx}$$

$$A_1 = G_2 - N_1$$

$$A_2 = G_2 + N$$

$$N = \frac{\sigma_o LB^2}{\rho_o u_o}$$

$$N_1 = \frac{a_1 BL}{\rho_o u_o^2}$$

$$N_2 = \frac{a_2 BL}{\rho_o u_o^2}$$

$$B_1 = - G_3 + 2G_1 + \frac{\gamma - 1}{\gamma} \frac{L}{\rho_o u_o} (\vec{J}\cdot\vec{E} - b_1)$$

$$B_2 = G_2 M^2(\gamma - 1) + \frac{\gamma - 1}{\gamma} \frac{L}{\rho_o u_o} (\vec{J}\cdot\vec{E} - b_2)$$

$$B_3 = - G_1 - \frac{\gamma - 1}{\gamma} \frac{L}{\rho_o u_o} b_3$$

$$\bar{\omega} = \bar{\omega}_1 + i\bar{\omega}_2 = \frac{\omega L}{u_o}$$

$$\bar{k} = kL$$

and L is a characteristic length which is taken to be one meter for the cases considered. In order for a nontrivial solution to exist for the set (49-51), the determinant of coefficients must equal zero. This results in a cubic equation in the complex frequency $\bar{\omega}$, i.e.

$$\bar{\omega}^3 + (- 3\bar{k} + iC_1)\bar{\omega}^2 + \left[\bar{k}^2(3 - \frac{1}{M^2}) + C_2 + i\bar{k}C_3\right] \bar{\omega} + \bar{k}^3(\frac{1}{M^2} - 1) + C_4\bar{k} + i\bar{k}^2C_5 + iC_6 = 0 \quad (52)$$

where the C's are real and depend on the steady-state variables. For a given steady-state solution satisfying Eqs. (6) through (8), and a given value of $\bar{k}$, the roots are determined using a computer program developed at AEDC for polynominals with complex coefficients. The criterion for instability is that the imaginary part of the root, $\bar{\omega}$, be greater than zero; i.e., $\bar{\omega}_2 > 0$. This implies that the disturbance can grow with respect to time at a given x station since

$$e^{i(kx-\omega_1 t)} = e^{i(kx-\omega_1 t)} e^{\omega_2 t}$$

It can be shown that when the steady-state gradient terms are zero and when there are no electrical effects present in the perturbed equations, there are three real roots (Ref. 13) of Eq. (52).

$$\omega = (u_o - a_o)k \tag{53}$$

$$\omega = u_o k \tag{54}$$

$$\omega = (u_o + a_o)k \tag{55}$$

The root $(u_o - a_o)k$ corresponds to a wave moving upstream relative to the gas at the sound speed while $(u_o + a_o)k$ is a wave moving downsteam relative to the gas at the sound speed. The root $u_o k$ corresponds to a wave moving with the gas and is identified as a perturbation in enthalpy. Landau and Lifshitz, Ref. 14, show that the entropy, vorticity, and enthalpy perturbations move with the gas velocity. In the presence of electromagnetic effects, the disturbances are found to be propagated at the speeds implied by Eqs. (53) through (55) when the wavelength is sufficiently short. These will be referred to as the upstream, downstream, and enthalpy modes. The disturbance velocity deviates from these values as the wavelength increases. It should be noted that the analysis is not valid at extremely short wavelengths because of the upper limit placed on the disturbance frequency by the Saha equilibrium assumption.

Using the steady-state solution shown in Fig. 3, the dispersion relation, Eq. (52), was solved at various points within the channel. The variation of $\bar{\omega}_2$ with x is shown in Fig. 4 for the enthalpy, upstream and downstream wave. Each point represents the local value of the growth rate and each point is calculated independent of the growth rate at any other x station. It can be seen that the enthalpy wave exhibits the largest instability ($\bar{\omega}_2 > 1$) and $\bar{\omega}_2$ for all three waves shows a marked dependence on the x position in the accelerator. Each x station corresponds to a different orientation of the wave front relative to the current vector as well as different values of the steady-state variables. The dependence of wave growth on wave orientation was indicated in Ref. 3 for the magneto-acoustic-type wave. It can be shown (Section 3.3) that the maximum joule heating occurs when the angle between the current vector and wave front is given approximately by $\epsilon_{max} = \frac{1}{2} \tan^{-1} \beta$. A plot of the angle between the wave front and current vector is shown in Fig. 5. The disturbance is oriented near the angle for maximum amplification at the channel entrance but the orientation becomes unfavorable for growth at subsequent downstream stations. The decreasing growth rate ($\bar{\omega}_2$) of the enthalpy wave with increasing x (Fig. 4) lends credence to the dependence on orientation. The strong variation of $\bar{\omega}$ with x is apparently attributable to the variation of the electrical quantities rather than the x dependence of the gas dynamic or thermodynamic variables.

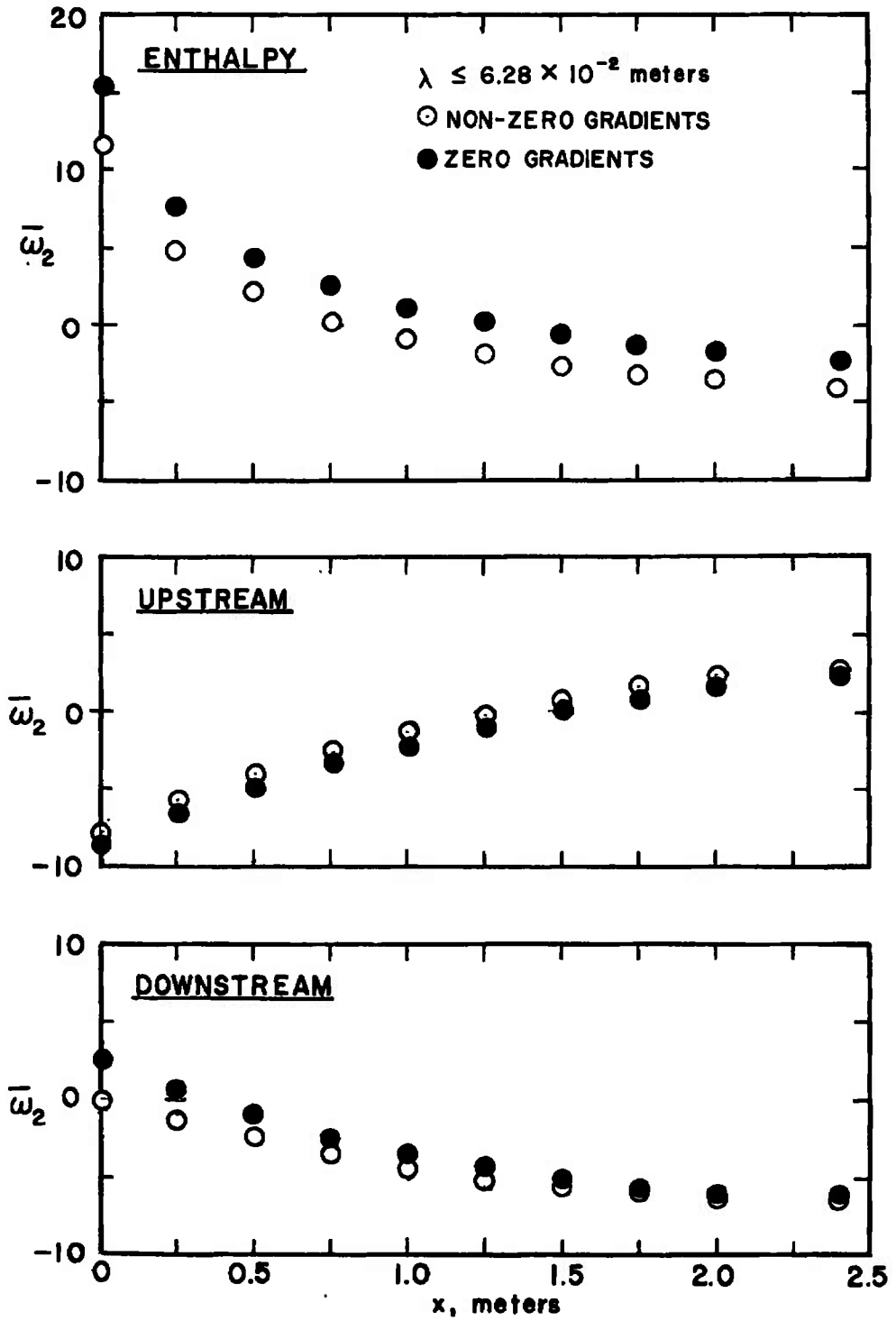

Fig. 4 Local Disturbance Growth Rate within Accelerator for Case I

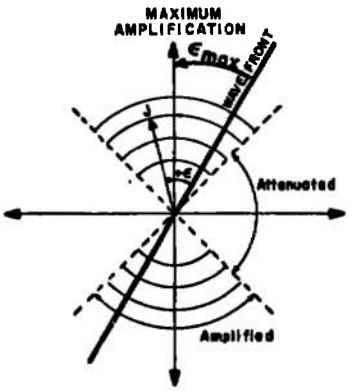

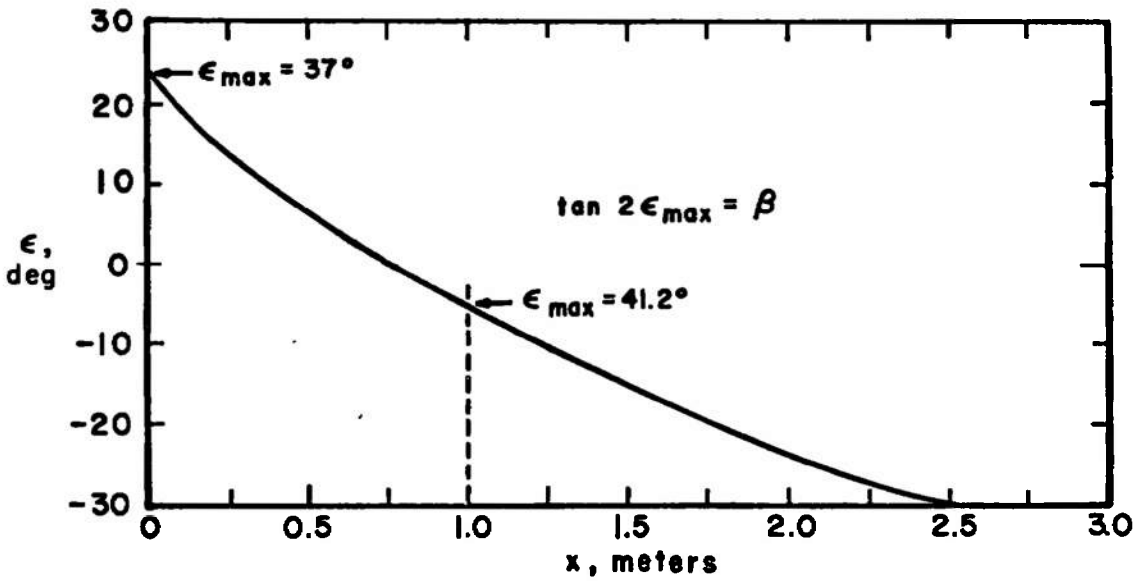

Fig. 5 Angle between Wave Front and Current Vector, $\epsilon = \tan^{-1}(-J_x/J_y)$

In order to determine the effects of the steady-state gradients, the quantities G_1, G_2, and G_3 were set to zero and Eq. (52) was solved for this case. Neglecting the gradient terms increases the value of $\bar{\omega}_2$ slightly for the enthalpy wave but does not change the general character of the x dependence as shown in Fig. 4. Reference 13 found a decrease in the growth when gradients were neglected in the generator analysis. The increase in growth attributable to the presence of gradients was attributed to the mechanism described by Morse (Ref. 15) for a three-fluid partially ionized plasma. This mechanism depends on the presence of an electric field either parallel or antiparallel to a density gradient and also on the mobility and diffusion of the electrons and ions within the gas. This mechanism is not dominant in accelerators or generators, but rather the gradients contribute convectively to the growth or decay of the waves. The contributions of the steady-state gradients to the wave growth rate were shown in Ref. 8 to be approximately

$$\mp\left[\frac{1 \mp (\gamma - 1 + M_o)}{1 \pm M_o}\right]\frac{L}{\rho_o}\frac{d\rho_o}{dx} \mp \frac{M_o}{2}\frac{L}{u_o}\frac{du_o}{dx}$$

where the upper sign refers to downstream waves and the lower sign to upstream waves. The contribution to the amplification or attenuation of a given wave depends only on the sign of the gradient.

The wavelength dependence of $\bar{\omega}_2$ and the nondimensional wave speed $\left(\frac{\bar{\omega}1}{\bar{k}} = \frac{u_{wave}}{u_o}\right)$ are shown in Figs. 6 and 7. It is noted that the waves travel at their nondispersive speeds for wavelengths less than approximately 0.1 m. The wave speeds show a marked deviation from their small interaction values at the longer wavelengths; however, at the longer wavelengths, the linearized theory breaks down and the complex frequency $\bar{\omega}$ can no longer be assumed to be, even approximately, independent of the x coordinate. The enthalpy wave $\bar{\omega}_2$ is noted to be almost independent of wavelength for short wavelengths, but then decreases for longer wavelengths. This is contrasted to the results of Ref. 6 where, because of heat conduction losses, the growth increases with wavelength.

The effect of thermal nonequilibrium on disturbance stability is investigated using the perturbation form of T_e given in Appendix I. The results for values of T_e up to 200°K higher than the gas temperature are shown in Fig. 8. The nonequilibrium effects are quite large at the entrance to the channel where the enthalpy wave shows the largest value of $\bar{\omega}_2$. It was found that ϕ_1 is zero for T_e - T between

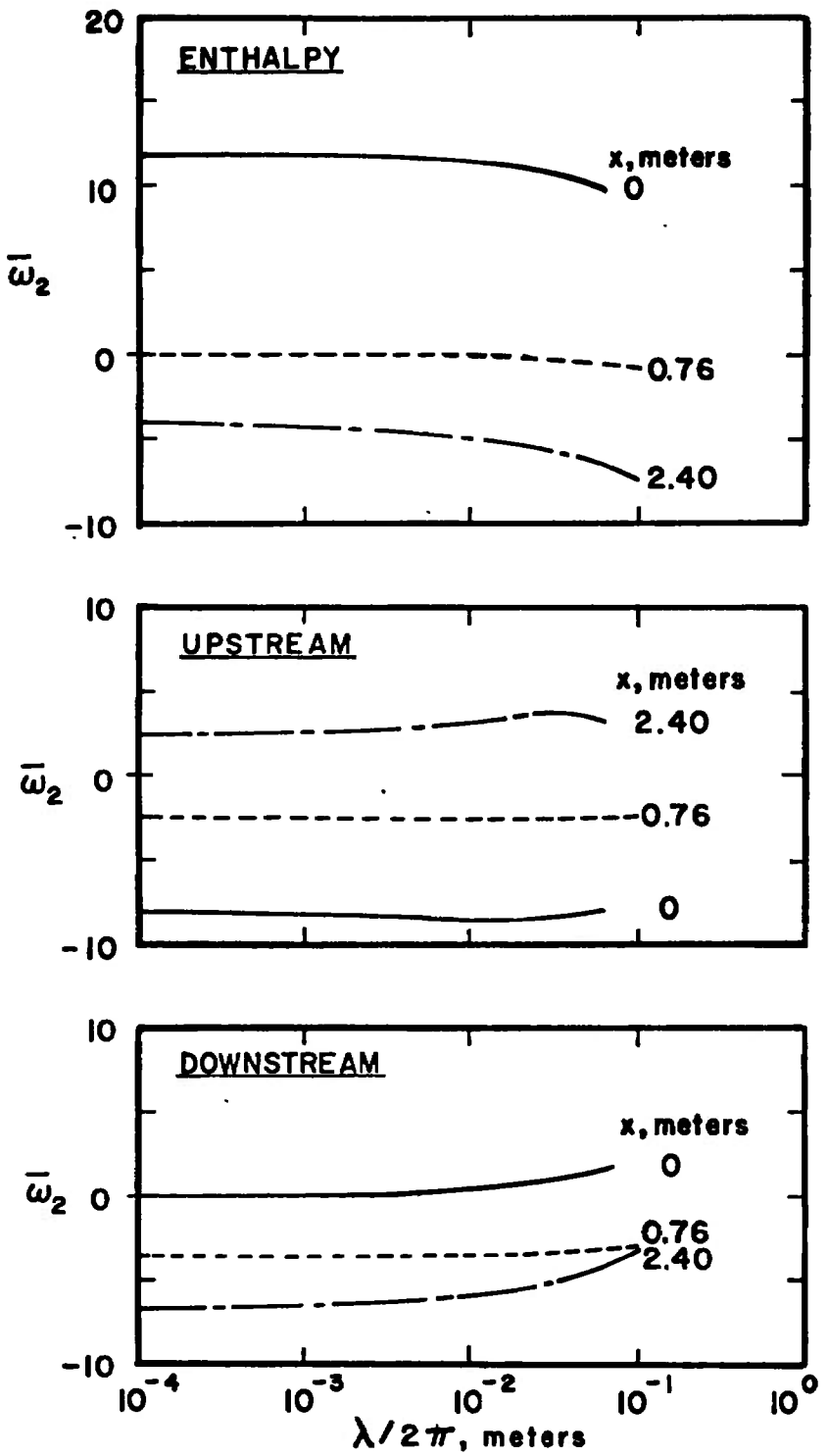

Fig. 6 Growth Rate versus Wavelength for Case I

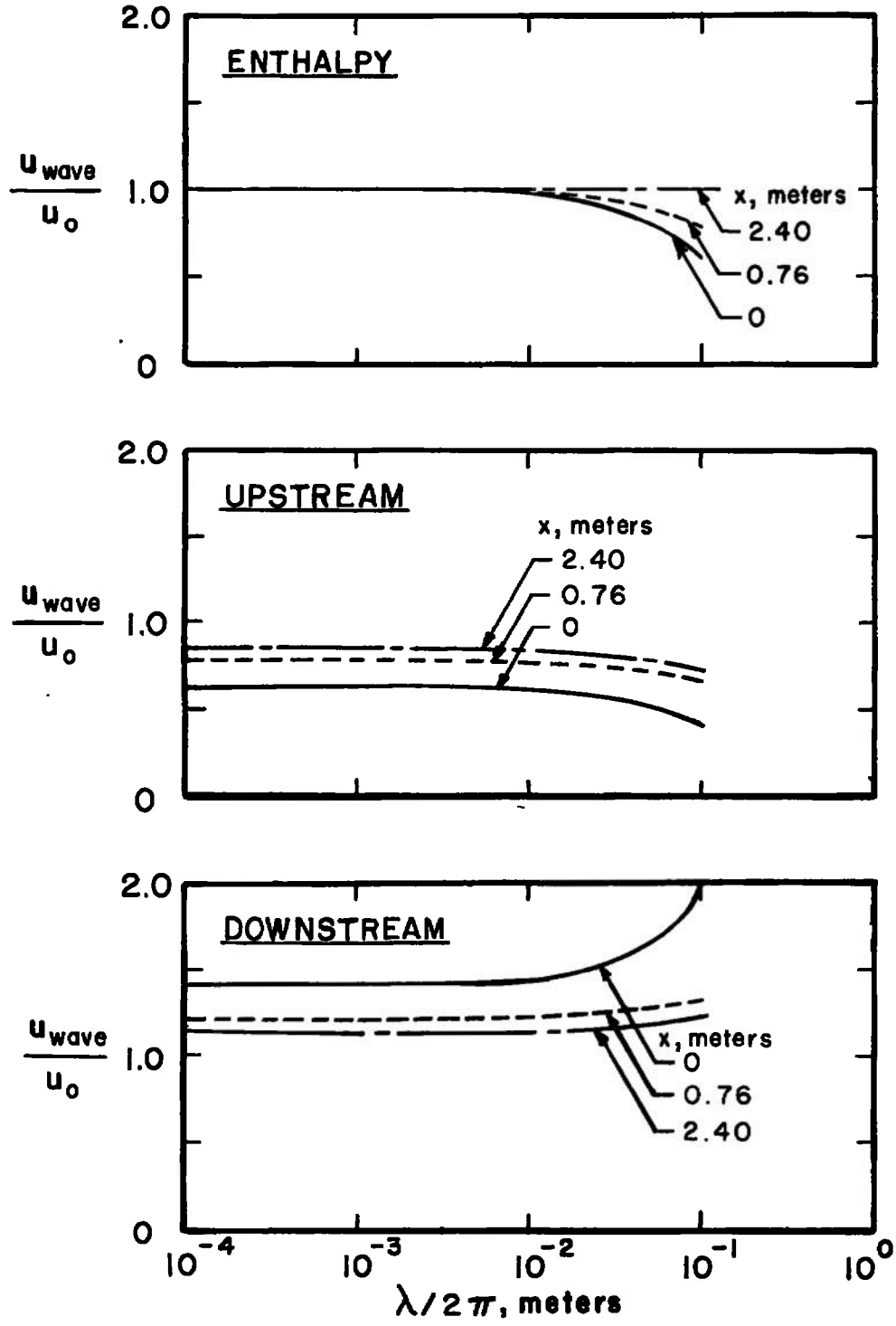

Fig. 7 Wave Speed versus Wavelength for Case I

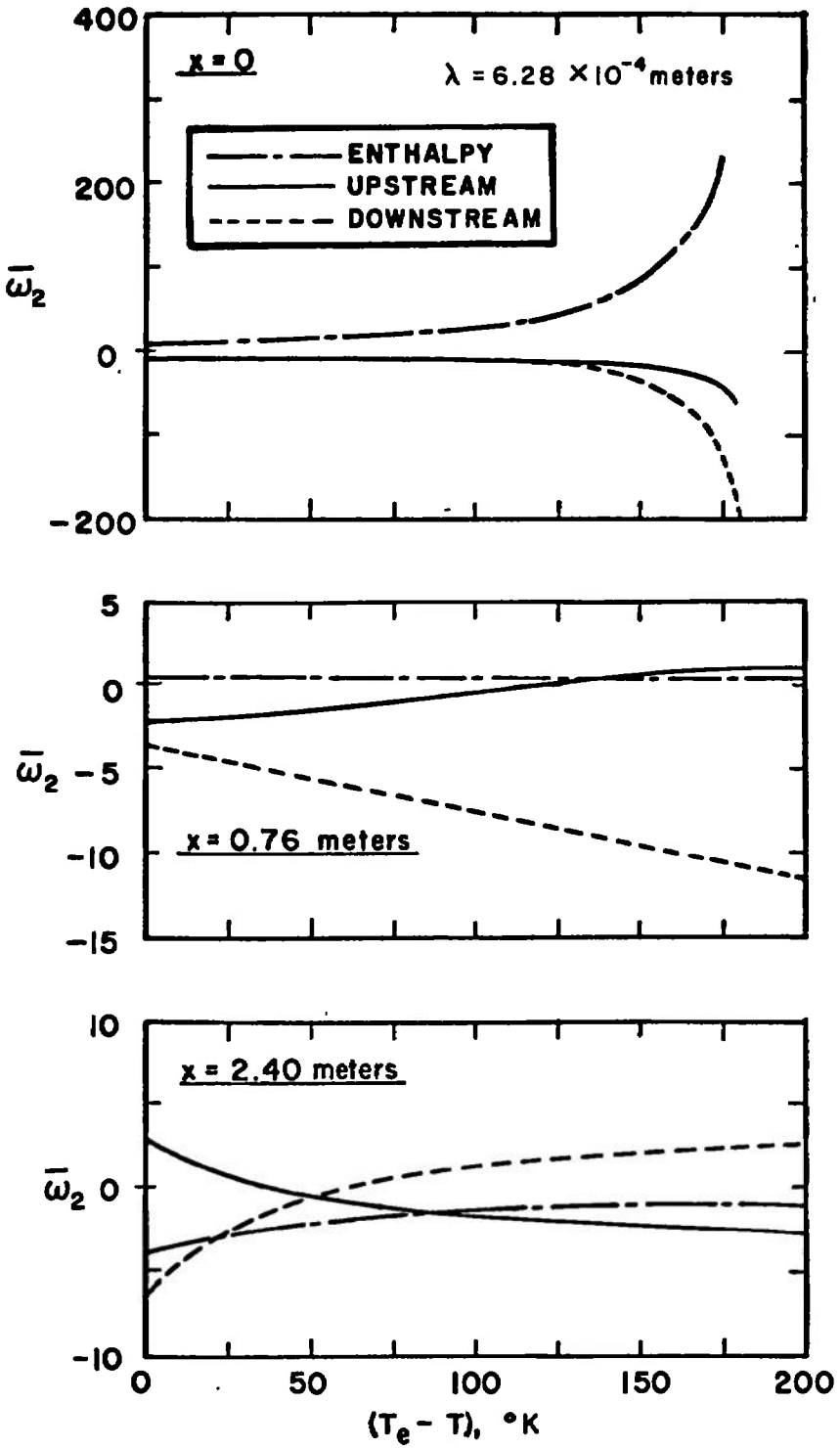

Fig. 8 Growth Rate versus Electron Temperature Elevation for Case I

185 and 190°K at x = 0.02. In this neighborhood the coefficients of the perturbed electron energy equation become unbounded and the linearized analysis breaks down. The nonequilibrium effects are quite different at different points within the channel. Reference 2 also showed that thermal nonequilibrium can markedly change the value of $\bar{\omega}_2$ for the upstream and downstream waves.

3.2 DISTURBANCE IN A BOUNDED PLASMA (CASE II)

The stability analysis of MHD slant-wall-type accelerator flows, assuming that $e_y = j_x = 0$, indicates that the enthalpy wave can become unstable and the disturbance may become large. The growth rate of the enthalpy wave is very dependent on the orientation of the current vector to the wave front. However, different assumptions within the stability analysis can lead to radically different results. If different boundary conditions are imposed on the perturbed electrical quantities, even though the same steady-state flow exists, different stability criteria will result.

Considering the case where the plasma is finite compared to the scale of the disturbance, the current density, j_y, and the joule heating, $\vec{E}_o \cdot \vec{j} + \vec{e} \cdot \vec{J}_o$, can again be related to u_1, p_1, and ρ_1. Making use of the conditions in Eqs. (43) and (44) the coefficients for the j_y expression given in Eq. (45) are

$$q_2 = \frac{\sigma_o u_o B}{1 + \Phi_o^2}$$

$$q_3 = - q_2$$

$$q_4 = \frac{\beta_o}{1 + \Phi_o^2} \frac{I}{A}$$

The coefficients of the perturbed joule heating term, Eq. (46), become

$$\gamma_1 = - \frac{I}{A} \left[E_x + \frac{u_o B(\beta_o - \Phi_o)}{1 + \Phi_o^2} \right]$$

$$\gamma_2 = \frac{I}{A} \left[\frac{1}{1 + \Phi_o^2} \left(\frac{I}{A} \frac{2\beta_o^2}{\sigma_o} - \beta_o u_o B \right) \right]$$

$$\gamma_3 = -\frac{I}{A}\frac{u_o B(\beta_o - \Phi_o)}{1 + \Phi_o^2} \tag{56}$$

The coefficients for the perturbed electron temperature given in Appendix I are the same except for q_1 which becomes

$$q_1 = \frac{2(J_y - \Phi_o J_x)}{J_y^2 - J_x^2}$$

The development of the dispersion relation follows as before with the dispersion relation, Eq. (52), as the result.

Using the steady-state solution shown in Fig. 3, $\bar{\omega}$ is determined as before with the results shown in Figs. 9 and 10. It is shown that the enthalpy and downstream waves are always damped whereas the upstream wave has a positive $\bar{\omega}_2$. The corresponding wave speeds have their nondispersive values at short wavelengths but diverge from these at longer wavelengths. The effects of thermal nonequilibrium are shown in Fig. 11. The higher electron temperature appears to move $\bar{\omega}_2$ toward the neutral stability point ($\bar{\omega}_2 = 0$) in the case considered.

It is shown that instabilities may exist with the wave amplification depending on the assumptions used in the analysis. When the perturbations in E_y and J_x were zero, the enthalpy wave was amplified and would grow by a factor of 10^5 in one meter if $\bar{\omega}_2$ remained constant at the initial value of 12. When the perturbations in E_y and J_x were non-zero, the upstream wave was amplified and would grow by a factor of 10^3 in a distance of one meter if $\bar{\omega}_2$ had a constant value of six. These growth factors can be taken only as an indication of the possible amplification, even at the short wavelengths, since contributions from nonlinear effects could become large and $\bar{\omega}_2$ is not independent of position in the channel. Electron thermal nonequilibrium is shown to have a marked effect on the growth when the plasma is infinite and very little effect when the accelerator walls influence the disturbance. Neglecting contributions from the steady-state gradients changed the magnitude of $\bar{\omega}_2$ only slightly.

3.3 APPROXIMATE ANALYSIS

Some insight into the contributing factors to instability can be obtained from an approximate analysis similar to that used in Ref. 3.

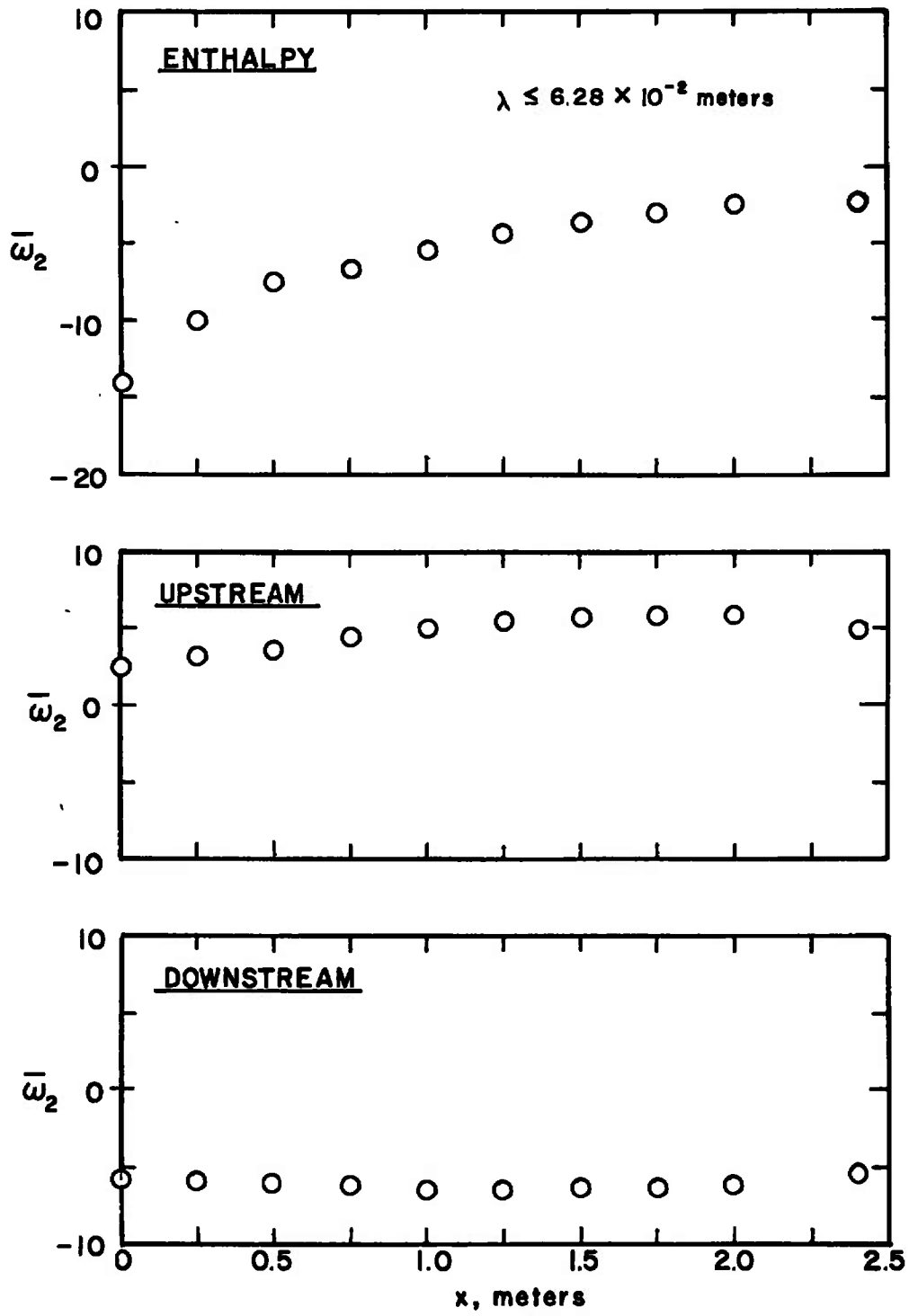

Fig. 9 Local Disturbance Growth Rate within the Accelerator for Case II

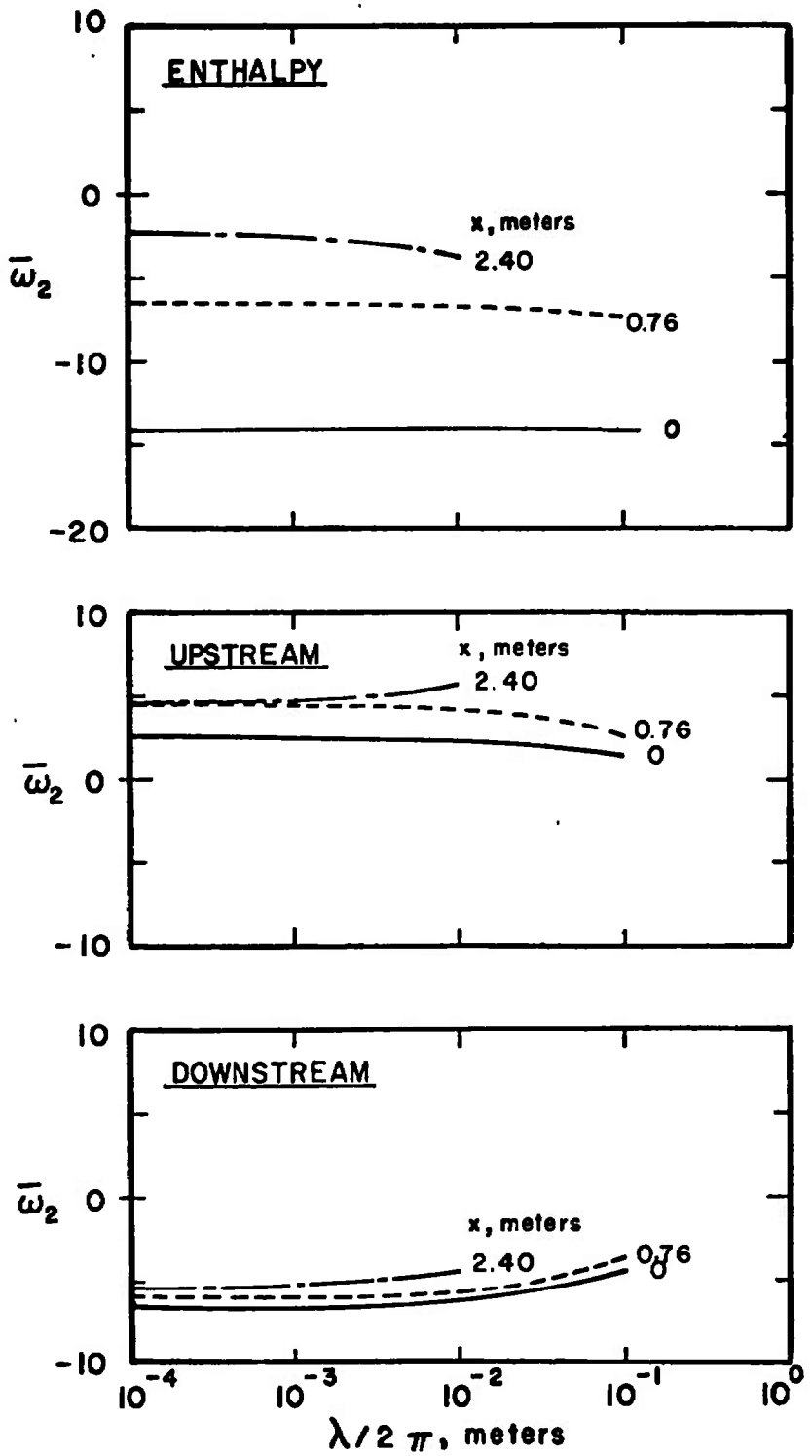

Fig. 10 Growth Rate versus Wavelength for Case II

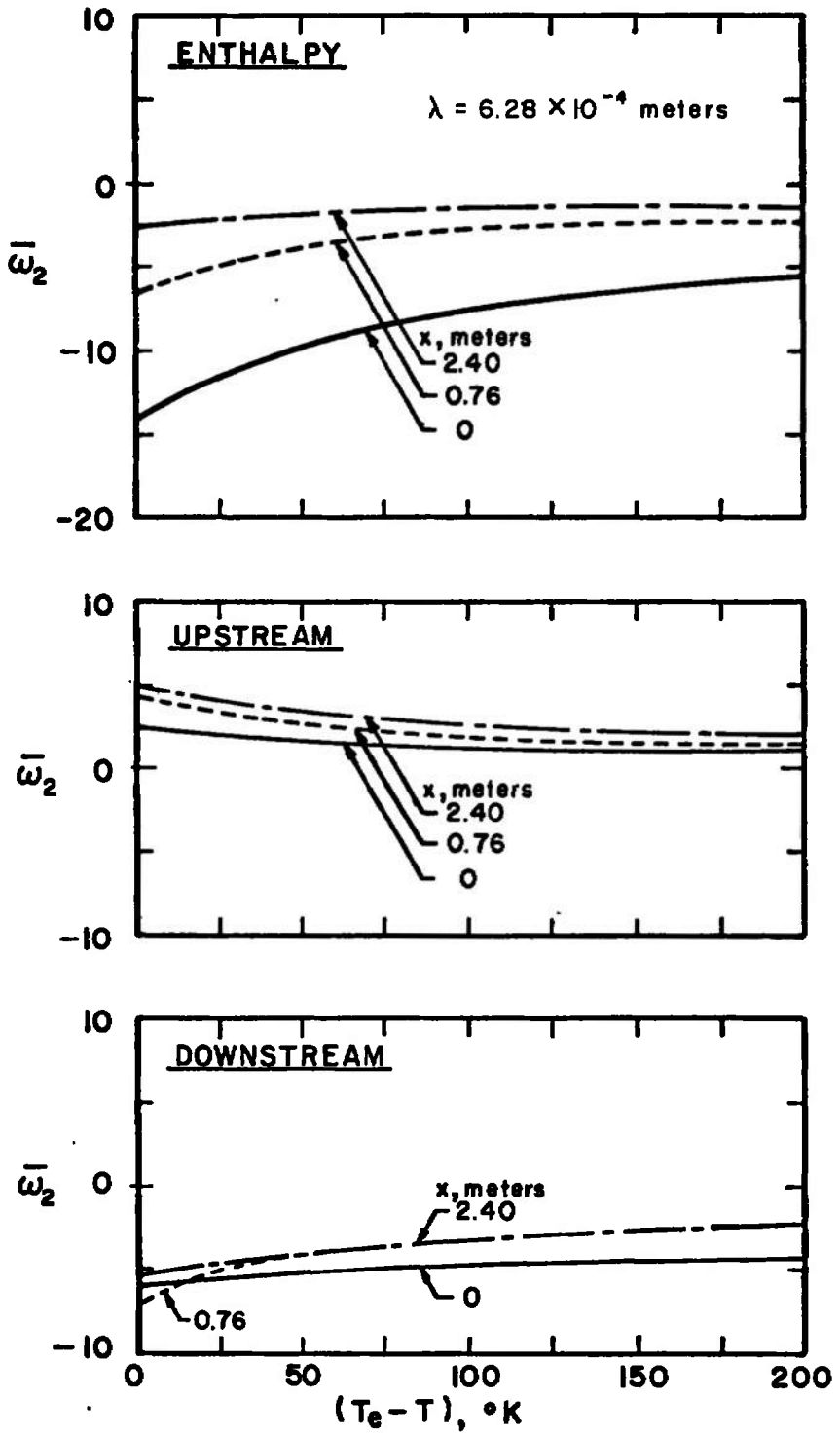

Fig. 11 Growth Rate versus Electron Temperature Elevation for Case II

Neglecting the steady-state gradient terms, the perturbed equations can be written as

$$\left(\frac{\bar{\omega} - \bar{k}}{\bar{k}}\right) \frac{\rho_1}{\rho_o} - \frac{u_1}{u_o} = 0 \tag{57}$$

$$\frac{i\,\bar{k}}{\gamma M^2} \frac{p_1}{p_o} - i(\bar{\omega} - \bar{k}) \frac{u_1}{u_o} = \frac{j_y\, BL}{\rho_o u_o^2} \tag{58}$$

$$- i(\bar{\omega} - \bar{k}) \frac{1}{\gamma M^2} \frac{p_1}{p_o} + \frac{i}{M^2} (\bar{\omega} - \bar{k}) \frac{\rho_1}{\rho_o} = \frac{(\gamma-1)L}{\rho_o u_o^3} \left\{ \frac{2(J_y + J_x \frac{j_x}{j_y}) j_y}{\sigma_o} - \frac{J_x^2 + J_y^2}{\sigma_o} \frac{\sigma_1}{\sigma_o} \right\} \tag{59}$$

where a different form of the energy equation is used. In order to obtain an approximate expression for $\bar{\omega}_2$, the right-hand side (RHS) of Eqs. (58) and (59) are computed using the adiabatic approximation $\frac{p_1}{p_o} = \gamma \frac{\rho_1}{\rho_o}$. Assuming constant collision cross sections, the perturbed conductivity and Hall coefficients can be written as

$$\frac{\beta_1}{\beta_o} = - \frac{\gamma + 1}{2} \frac{\rho_1}{\rho_o}$$

$$\frac{\sigma_1}{\sigma_o} = \left[\frac{eV_i}{2kT}(\gamma - 1) + \frac{\gamma - 3}{4} \right] \frac{\rho_1}{\rho_o} = R_\sigma \frac{\rho_1}{\rho_o} \tag{60}$$

Using the adiabatic approximation and Eqs. (57) and (60), the RHS of Eq. (58) can be written as

$$\frac{BL}{\rho_o u_o^2} j_y = \frac{BL}{\rho_o u_o^2} \left\{ - q_2 \left(\frac{\bar{\omega} - \bar{k}}{\bar{k}}\right) + q_3 R_\sigma - q_4 \frac{\gamma + 1}{2} \right\} \frac{\rho_1}{\rho_o}$$

$$= F \frac{\rho_1}{\rho_o} = (F_r + iF_i) \frac{\rho_1}{\rho_o} \tag{61}$$

The RHS of Eq. (59) can be written as

$$\frac{(\gamma-1)L}{\sigma_o \rho_o u_o^3}\left\{2F\left(\frac{\rho_o u_o^2}{BL}\right)\left[J_y + \left(\frac{j_x}{j_y}\right)J_x\right] - R_\sigma\left(J_x^2 + J_y^2\right)\right\}\frac{\rho_1}{\rho_o}$$

$$= D\,\frac{\rho_1}{\rho_o} = (D_r + iD_i)\,\frac{\rho_1}{\rho_o} \tag{62}$$

Combining Eqs. (57) through (62), the condition for a nontrivial solution is

$$\gamma + \frac{iD}{\bar{\omega} - \bar{k}} + \frac{\gamma M^2}{\bar{k}}\left(iF - \frac{(\bar{\omega} - \bar{k})^2}{\bar{k}}\right) = 0$$

Approximating $(\bar{\omega} - \bar{k})$ in the term $iD/(\bar{\omega} - \bar{k})$ by $\pm\bar{k}/M$ (which is regarded as an iteration in solving the cubic in $\bar{\omega}$) an approximate expression for $\bar{\omega}_2$ can be written as

$$\bar{\omega}_2 = \frac{D_r}{2\gamma} \pm \frac{M}{2} F_r \tag{63}$$

The upper sign corresponds to the downstream wave and the lower sign refers to the upstream wave. Because of the various approximations, the root corresponding to the enthalpy wave has been eliminated.

The expression for $\bar{\omega}_2$ when $e_y = j_x = 0$ can be written as

$$\bar{\omega}_2 = \frac{\sigma_o B^2 L}{2\rho_o u_o}\left\{-1 \pm \frac{J_y M}{\sigma_o u_o B}\left[(R_\sigma - 2(\gamma-1)\right] \mp \frac{\beta_o M J_x}{\sigma_o u_o B}\left(R_\sigma + \frac{\gamma+1}{2}\right)\right.$$

$$\left. + \frac{M^2(\gamma-1)}{\sigma_o^2 u_o^2 B^2}\left(J_y^2 - J_x^2\right)R_\sigma - \frac{2\beta_o J_y J_x M^2(\gamma-1)}{\sigma_o^2 u_o^2 B^2}\left(R_\sigma + \frac{\gamma+1}{2}\right)\right\} \tag{64}$$

All terms in Eq. (64), except for the last term, are identified in Eqs. (39) and (40) of Ref. 3. The last term is a coupling term required by the presence of two components of current in the joule heating term, D_r. A plot of Eq. (64) using the steady-state solution

of Fig. 3 is shown in Fig. 12a. Comparison of Fig. 12a with Fig. 4 for the upstream and downstream wave shows that the simplifying assumptions and approximations made in arriving at Eq. (64) affect the magnitude of $\bar{\omega}_2$ slightly but do not alter the character of the x dependence. The growth or decay of the waves is shown to be very dependent on the magnitude (and sign) of J_x and J_y. The largest contribution to instability comes from the third term which contains the axial current density, J_x. As in previous analyses (e.g., Refs. 3 and 7) the wave propagating antiparallel to the current vector is amplified. Since J_x goes through zero, the downstream wave is amplified near the channel entrance, but the upstream wave is amplified near the exit.

The angle between the current vector and the wave front (see Fig. 5) which gives the maximum growth rate can be calculated from Eq. (64). The body force terms (second and third terms of Eq. (64)) are a maximum when

$$\tan \epsilon = \beta \left(\frac{R_\sigma + \frac{\gamma+1}{2}}{R_\sigma - 2(\gamma-1)} \right)$$

The joule heating terms (last two terms of Eq. (64)) are a maximum when

$$\tan 2\epsilon = \beta \left(\frac{R_\sigma + \frac{\gamma+1}{2}}{R_\sigma} \right)$$

The maximum contribution from the body force terms occurs when the angle between the current vector and wave front is approximately 86 deg. Since the force terms are larger than the joule heating terms, this orientation will give the maximum growth rate. As can be seen from Fig. 5, this optimum orientation is not present, and axially moving acoustic waves are not significantly amplified.

The expression for $\bar{\omega}_2$ when $e_y = \Phi_o e_x$ and $j_x = -\Phi_o j_y$ can be written as

$$\bar{\omega}_2 = \frac{\sigma_o B^2 L}{2\rho_o u_o (1+\Phi_o^2)} \left\{ -1 \mp MR_\sigma \mp \frac{\gamma+1}{2} \frac{\beta_o M}{\sigma_o u_o B} \left(\frac{I}{A}\right) \right.$$

$$+ \frac{2M(\gamma-1)(J_y - \bar{\Phi}_o J_x)}{\sigma_o u_o B}\left[\mp 1 - MR_\sigma - \frac{\gamma+1}{2}\frac{\beta_o M}{\sigma_o u_o B}\left(\frac{I}{A}\right)\right]$$

$$- \frac{M^2(\gamma-1)(1+\bar{\Phi}_o^2)(J_x^2 + J_y^2)}{\sigma_o^2 u_o^2 B^2} R_\sigma \Bigg\} \qquad (65)$$

The first three terms are related to fluctuations in the forcing term, F_r, and the remaining terms are related to changes in the joule heating. A plot of $\bar{\omega}_2$ versus x for this case is shown in Fig. 12b using the steady-state solution of Fig. 3. The result is very similar to that obtained by solving the cubic dispersion relation (Fig. 9). The largest contribution comes from the perturbation in the forcing term, F_r, i.e., the second and third terms of Eq. (65). The body force term is independent of the orientation of the wave front to the current vector. The contribution from joule heating decreases as x increases and is negligible at the end of the channel.

The growth of the enthalpy wave can be calculated approximately by considering the growth of a stationary enthalpy disturbance attributable to joule heating. It is assumed that the disturbance is a plane wave so that $e_y \equiv j_x \equiv 0$ corresponding to Case I. The perturbed energy equation takes the simple approximate form

$$\rho_o \frac{\partial h_1}{\partial t} = \frac{2 j_y J_y}{\sigma_o} - \frac{\sigma_1}{\sigma_o} J^2 \qquad (66)$$

Using Eqs. (9) and (10), the perturbed current density can be written as

$$j_y = \frac{\sigma_1}{\sigma_o}(J_y - \beta_o J_x) + \frac{\beta_1}{\beta_o}\beta_o J_x \qquad (67)$$

It is assumed that the electrical conductivity and Hall coefficient can be written as power law functions of the enthalpy; i.e.

$$\frac{\sigma_1}{\sigma_o} = w_1 \frac{h_1}{h_o} \qquad (68)$$

$$\frac{\beta_1}{\beta_o} = w_2 \frac{h_1}{h_o} \tag{69}$$

Using Eqs. (66) through (69), the perturbation energy equation can be written as

$$\frac{L}{u_o} \frac{\partial \ell n h_1}{\partial t} = \frac{L}{u_o} \left(\frac{1}{\sigma}\right) \frac{\gamma - 1}{\gamma p} w_1 \left\{ J_y^2 - J_x^2 - \beta_o J_x J_y \left(1 - \frac{w_2}{w_1}\right) \right\} \tag{70}$$

using perfect gas relations.

The right-hand side of Eq. (70) has been nondimensionalized using the free-stream velocity so that it now corresponds to the temporal growth rate, $\bar{\omega}_2$. It is shown that the first term of Eq. (70) is always destabilizing since $J_y > J_x$, and the second term is destabilizing when J_x is negative since, in general, $w_1 > w_2$. Using $w_1 = 6$ and $w_2 = 1$, the approximate enthalpy growth rate is calculated from Eq. (70) using the steady-state solution of Fig. 3. The growth rate is shown in Fig. 13. A comparison of Fig. 13 with Fig. 4 shows that Eq. (70) underestimates the value of the growth rate at the accelerator entrance but does qualitatively predict the growth rate distribution through the accelerator.

The angle for maximum enthalpy growth can be found from Eq. (70) by relating the current components to the angle between the wave front and current vector (defined in Fig. 5). The current components can be written as

$$J_y = J \cos \varepsilon \tag{71}$$

$$J_x = - J \sin \varepsilon \tag{72}$$

Using Eqs. (71) and (72) in Eq. (70), the approximate expression for the growth rate can be written as

$$\frac{L}{u_o} \frac{\partial \ell n h_1}{\partial t} = \frac{L}{u_o} \left(\frac{J^2}{\sigma}\right) \left(\frac{\gamma - 1}{\gamma p}\right) w_1 \left\{ \cos 2\varepsilon + \beta_o \sin 2\varepsilon \left(1 - \frac{w_2}{w_1}\right) \right\} \tag{73}$$

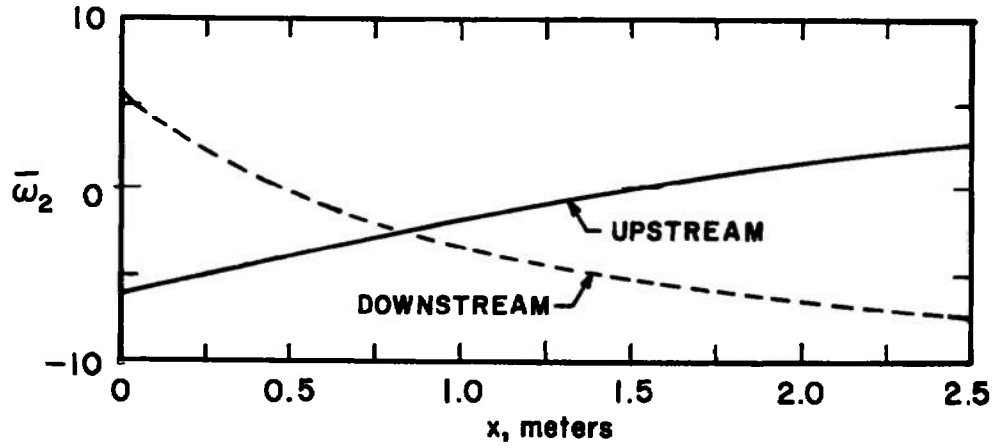

a. Case I

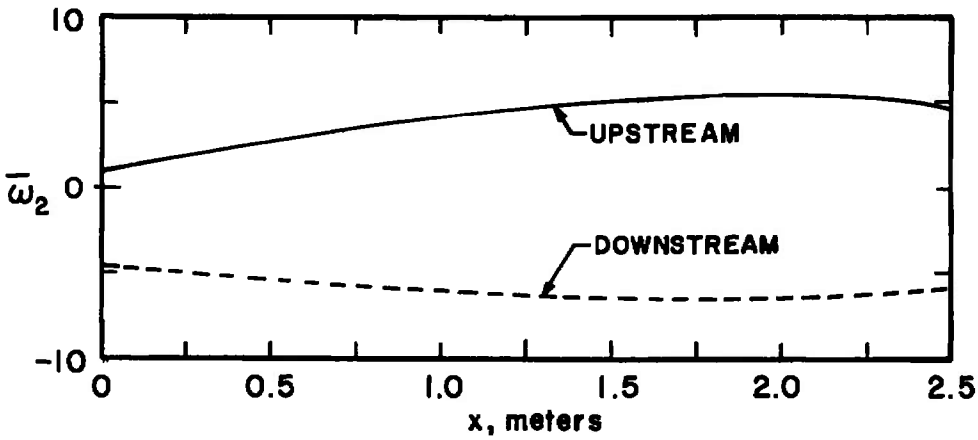

b. Case II

Fig. 12 Approximate Growth Rate of Magneto-Acoustic Waves as a Function of x

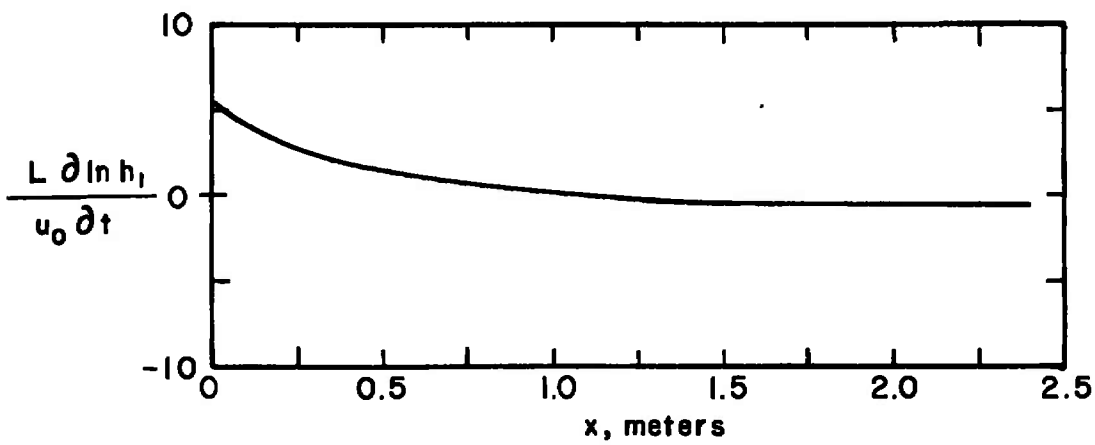

Fig. 13 Approximate Growth Rate of Enthalpy Waves as a Function of x for Case I

The angle for maximum growth is then found from Eq. (73) as

$$\tan 2\epsilon = \beta_o\left(1 - \frac{w_2}{w_1}\right) \tag{74}$$

where the term w_2/w_1 represents the contribution from the perturbed Hall coefficient which is stabilizing. The orientation most favorable for growth is near the channel entrance, and the wave orientation becomes less favorable for growth as x increases. This trend agrees with the growth rates predicted from the Case I analysis.

The approximate results shown here, together with the results from the previous cases ($e_y = j_x = 0$ and $e_y = \Phi_o e_x$; $j_x = -\Phi_o j_y$) indicate that instabilities may exist in slant-wall accelerators. Although the linearized analysis is inadequate for predicting the disturbance growth and is restricted to short wavelength, insight is gained into the instability mechanism. It is shown that different assumptions concerning the electrical boundary conditions give radically different results for stability criteria. In an attempt to remove some of the restrictions in the analysis, a two-dimensional perturbation model is considered in the next section.

SECTION IV
TWO-DIMENSIONAL ANALYSIS

The perturbation variables must satisfy Eqs. (17) through (20) together with the conditions imposed by Eqs. (36) through (39). Previously, it has been assumed that the imposed disturbances are axial traveling waves which depend only on x and t. This restriction will be relaxed to investigate the stability of traveling waves which are dependent on the transverse coordinate, y, as well as x and t. This approach permits a more realistic treatment because the perturbed y momentum equation is not neglected and the waves are not restricted to propagate only in the x direction.

The conditions $\nabla \times \vec{e} = 0$ and $\nabla \times \vec{v} = 0$ imply that the perturbed electric field and velocity are derivable from potential functions. Hence

$$\vec{e} = -\nabla V$$
$$\vec{v}_\perp = \nabla \varphi \tag{75}$$

It is assumed that

$$V \sim e^{i(k_x x + k_y y - \omega t)}$$
$$\varphi \sim e^{i(k_x x + k_y y - \omega t)} \tag{76}$$

The components of perturbed electric field and velocity can now be expressed as

$$e_x = - ik_x V$$
$$e_y = - ik_y V$$
$$u_1 = ik_x \varphi$$
$$v_1 = ik_y \varphi \tag{77}$$

The conservation of current, $\nabla \cdot \vec{j} = 0$, implies that $\vec{j}$ can be expressed as

$$j_x = \frac{\partial \psi}{\partial y}$$
$$j_y = - \frac{\partial \psi}{\partial x} \tag{78}$$

McCune (Ref. 3) used Eqs. (75) and (78), together with Ohm's law and the momentum and continuity equations, to determine a set of differential equations which together with appropriate boundary conditions determine V, ϕ, ψ, and p. The energy equation was eliminated by noting that dissipation terms are much smaller than the body force terms for the case considered and, hence, the adiabatic approximation $\left(\frac{p_1}{p_o} = \gamma \frac{\rho 1}{\rho_o}\right)$ can be used. The adiabatic approximation is not made in this analysis and conservation of current is not satisfied exactly. Ohm's law is used to establish the relation between ψ, ϕ, V, and p. Equations (17) through (20) can in principle be solved for ϕ, V, ρ, and p and then ψ can be determined from Ohm's law.

The assumed form of the perturbations, Eq. (76), implies that the medium is infinite, compared to the scale of the disturbance, in both x and y direction. It is not possible, then, to treat reflection or attenuation of a disturbance at the accelerator walls. However, the initial

development of the disturbance can be investigated and the analysis can be used to determine if the necessary conditions for instability are present.

The perturbed Ohm's law, Eqs. (21) and (22), can be written as

$$j_x = \frac{\partial \psi}{\partial y} = - ik_x \sigma_{ef} V + ik_y \beta_o \sigma_{ef} V + ik_y \sigma_{ef} B\varphi + i\sigma_{ef}\beta_o B k_x \varphi + J_x \frac{\sigma_1}{\sigma_o} - \beta_{ef}(J_y + \beta_o J_x)\frac{\beta_1}{\beta_o} \tag{79}$$

$$j_y = - \frac{\partial \psi}{\partial x} = - ik_y \sigma_{ef} V - ik_x B \sigma_{ef} \varphi - ik_x \beta_o \sigma_{ef} V + ik_y \beta_o B \sigma_{ef} \varphi + J_y \frac{\sigma_1}{\sigma_o} + \beta_{ef}(J_x - \beta_o J_y)\frac{\beta_1}{\beta_o} \tag{80}$$

The expressions for j_x and j_y are used together with the perturbed joule heating

$$(\vec{J} \cdot \vec{E})_1 = J_x e_x + J_y e_y + E_x j_x + E_y j_y \tag{81}$$

and the expressions given in Appendix I for the perturbed conductivity and Hall coefficient to express Eqs. (17) through (20) in terms of ϕ, V, p,. and ρ.

The perturbed equations can now be written as

$$A_1 \frac{\rho_1}{\rho_o} + \left\{ - A_3 + i\bar{k}_x P \right\} \frac{p_1}{p_o} + \left\{ i(N_{ef}\bar{k}_y + \bar{k}_x \beta_o N_{ef}) \right\} \frac{V}{u_o BL} + \left\{ \bar{k}_x \bar{\omega} - \bar{k}_x^2 - i(\beta_o N_{ef} \bar{k}_y - \bar{k}_x A_2) \right\} \frac{\varphi}{u_o L} = 0 \tag{82}$$

$$E_1 \frac{\rho_1}{\rho_o} + \left\{ E_3 + i\bar{k}_y P \right\} \frac{p_1}{p_o} + \left\{ i(\beta_o N_{ef} \bar{k}_y - \bar{k}_x N_{ef}) \right\} \frac{V}{u_o BL} + \left\{ \overline{\omega k_y} - \bar{k}_x \bar{k}_y + i(\bar{k}_y N_{ef} + \bar{k}_x E_2) \right\} \frac{\varphi}{u_o L} \tag{83}$$

$$\left\{-G_1 + i(\bar{k}_x - \bar{\omega})\right\}\frac{\rho_1}{\rho_o} + \frac{\varphi_1}{u_o L}\left\{-\bar{k}_x^2 - \bar{k}_y^2 + i\bar{k}_x G_1\right\} = 0 \qquad (84)$$

$$\left\{B_1 + i(\bar{\omega} - \bar{k}_x)\right\}\frac{\rho_1}{\rho_o} + \left\{B_3 + i\left(\bar{k}_x - \frac{\bar{\omega}}{\gamma}\right)\right\}\frac{p_1}{p_o}$$
$$+ \left\{-i(\bar{k}_y b_4 + i\bar{k}_x b_2)\right\}\frac{V_1}{u_o BL} + \left\{(\bar{k}_x\bar{\omega} - \bar{k}_x^2)\, M^2(\gamma-1)\right.$$
$$\left. - i(\bar{k}_y b_3 - \bar{k}_x B_2)\right\}\frac{\varphi_1}{u_o L} = 0 \qquad (85)$$

where the following new definitions are made

$$N_{ef} = \frac{\sigma_{ef}\, B^2 L}{\rho_o u_o} \qquad P = \frac{p_o}{\rho_o u_o^2}$$

$$F_y = \frac{J_y\, BL}{\rho_o u_o^2} \qquad F_x = \frac{J_x\, BL}{\rho_o u_o^2}$$

$$A_1 = G_2 - F_y\xi_2 - \mu_3\beta_{ef}(F_x - \beta_o F_y)$$

$$A_2 = G_2 + N_{ef} - F_y\xi_3 - \mu_4\beta_{ef}(F_x - \beta_o F_y)$$

$$A_3 = F_y\xi_1 + \mu_2\beta_{ef}(F_x - \beta_o F_y)$$

$$E_1 = \xi_2 F_x - \mu_3\beta_{ef}(F_y + \beta_o F_x)$$

$$E_2 = \beta_o N_{ef} + F_x\xi_3 - \mu_4\beta_{ef}(F_y - \beta_o F_x)$$

$$E_3 = \xi_1 F_x - \mu_2\beta_{ef}(F_y + \beta_o F_x)$$

$$b_1 = \frac{\gamma-1}{\gamma}\frac{L}{p_o u_o}\left\{(\xi_2 - \beta_o\beta_{ef}\mu_3)\vec{J}\cdot\vec{E} + \beta_{ef}\mu_3(E_yJ_x - E_xJ_y)\right\}$$

$$b_2 = \frac{\gamma-1}{\gamma}\frac{L}{p_o}\left\{-B\left[J_x + \sigma_{ef}(E_x + \beta_o E_y)\right]\right\}$$

$$b_3 = \frac{\gamma-1}{\gamma}\frac{L}{p_o u_o}\left\{(\xi_1 - \beta_o\beta_{ef}\mu_2)\vec{J}\cdot\vec{E} + \beta_{ef}\mu_2(E_yJ_x - E_xJ_y)\right\}$$

$$b_4 = \frac{\gamma-1}{\gamma}\frac{L}{p_o}\left\{-J_yB + \sigma_{ef}B(\beta_o E_x - E_y)\right\}$$

$$b_5 = \frac{\gamma-1}{\gamma}\frac{L}{p_o u_o}\left\{(\xi_3 - \beta_o\beta_{ef}\mu_4)\vec{J}\cdot\vec{E} + \mu_4\beta_{ef}(E_yJ_x - E_xJ_y) + \sigma_{ef}\,B\,u_o(\beta_o E_x - E_y)\right\}$$

$$b_6 = \frac{\gamma-1}{\gamma}\frac{L}{p_o}\left\{\sigma_{ef}\,B(E_x + \beta_o E_y)\right\}$$

$$B_1 = 2G_1 - G_3 + \vec{J}\cdot\vec{E}\left(\frac{\gamma-1}{\gamma}\frac{L}{p_o u_o}\right) - b_1$$

$$B_2 = M^2(\gamma-1)G_2 + \vec{J}\cdot\vec{E}\left(\frac{\gamma-1}{\gamma}\frac{L}{p_o u_o}\right) - b_5$$

$$B_3 = -G_1 - b_3 \tag{86}$$

The dispersion relation is obtained by setting the determinant of coefficients of the algebraic set of equations, Eqs. (82) through (85) to zero. After considerable algebraic manipulations, the resulting dispersion relation is of the form

$$CA_1\bar{\omega}^3 + (CA_2 + iCB_2)\bar{\omega}^2 + (CA_3 + iCB_3)\bar{\omega} + CA_4 + iCB_4 = 0 \tag{87}$$

The dispersion relation is again a cubic and in the absence of electromagnetic effects reduces to the equations for traveling acoustic and enthalpy waves. The steady-state solution shown in Fig. 3 is utilized with the investigation restricted to thermal equilibrium; that is, $T_e = T$.

It is seen from Fig. 14 that for wavelength in the y direction greater than 0.1 m and for large values of k_x, the growth rate reduces to that obtained from the one-dimensional analysis with $e_y = e_x = 0$ (Fig. 4). This was expected since as $k_y \rightarrow 0$ the gradients in the y direction are eliminated. Also, in both cases the perturbation of slant angle and total current are nonzero, whereas in the case where $e_y = \Phi_o e_x$ and $j_x = -\Phi_o j_y$, they were assumed zero. However, the two-dimensional perturbation analysis has $j_x \neq 0$, but this finite perturbation in the axial current does not change the stability results for short wavelengths.

The growth rate for the various waves is plotted versus axial wavelength in Fig. 15 and versus k_y in Fig. 16. The growth rate for the enthalpy wave is shown to decrease for increasing λ_x and decreasing λ_y. The growth rate for the upstream wave increases slightly for increasing λ_x and decreasing λ_y, but the opposite is true for the downstream wave. Changing λ_x (or λ_y) is equivalent to changing the wave orientation in the flow, with the angle between the current vector and wave front given by

$$\tan \epsilon = \frac{-\frac{J_x}{J_y} - \frac{\lambda_x}{\lambda_y}}{1 - \frac{J_x}{J_y}\frac{\lambda_x}{\lambda_y}}$$

Then, at the accelerator entrance, increasing λ_x/λ_y corresponds to a decreasing angle and a less favorable condition for amplification of the enthalpy wave.

The wave speed dependence on wavelength is shown in Fig. 17. As before, the waves deviate from their nondispersive velocities at wavelengths (λ_x) on the order of 0.1 m. The wave speeds of the upstream and downstream waves deviate at smaller values of λ_x as the wavelength in the y direction decreases below one meter.

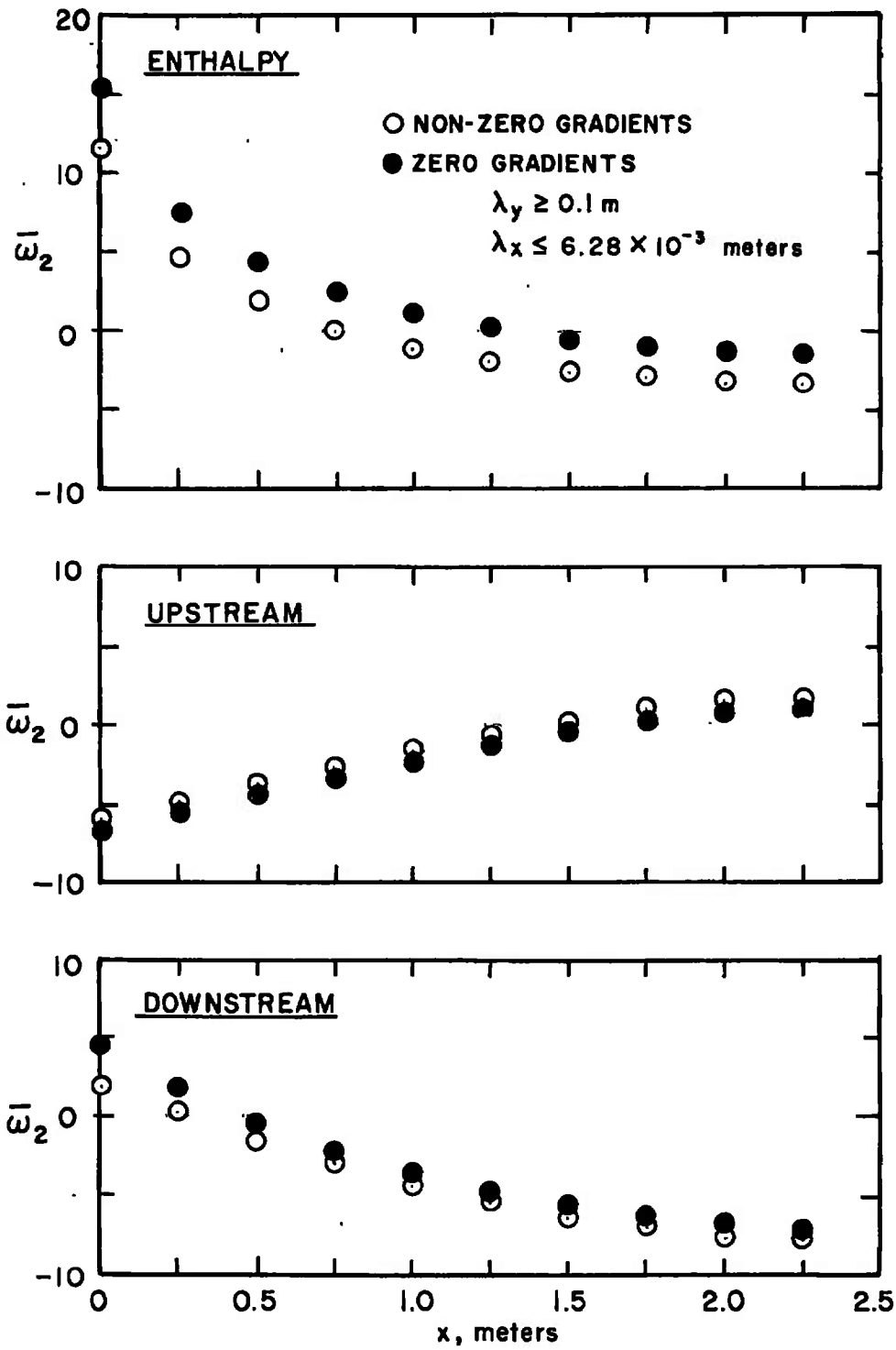

Fig. 14 Local Growth Rate of a Two-Dimensional Disturbance as a Function of Axial Position

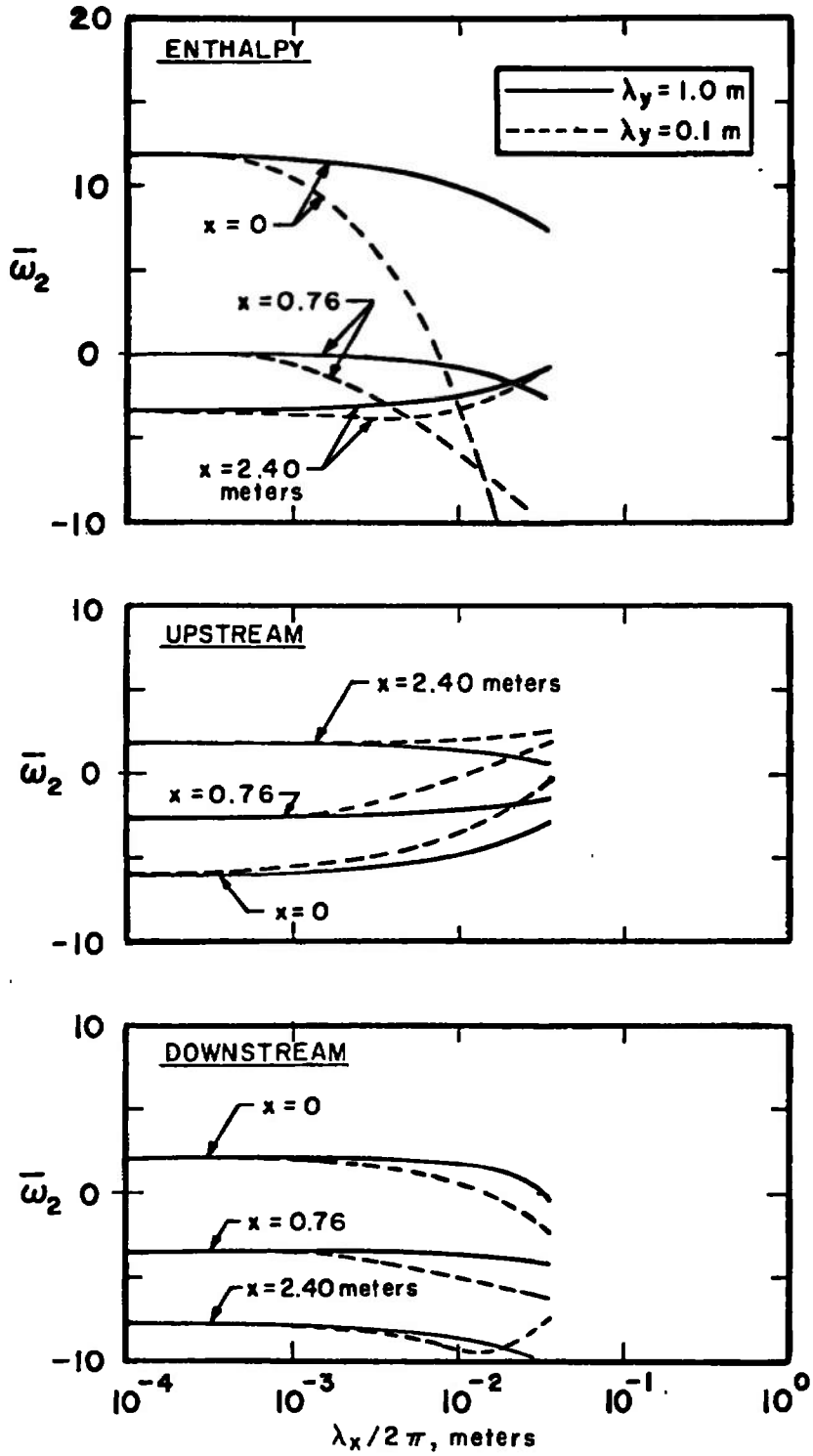

Fig. 15 Growth Rate versus Axial Wavelength

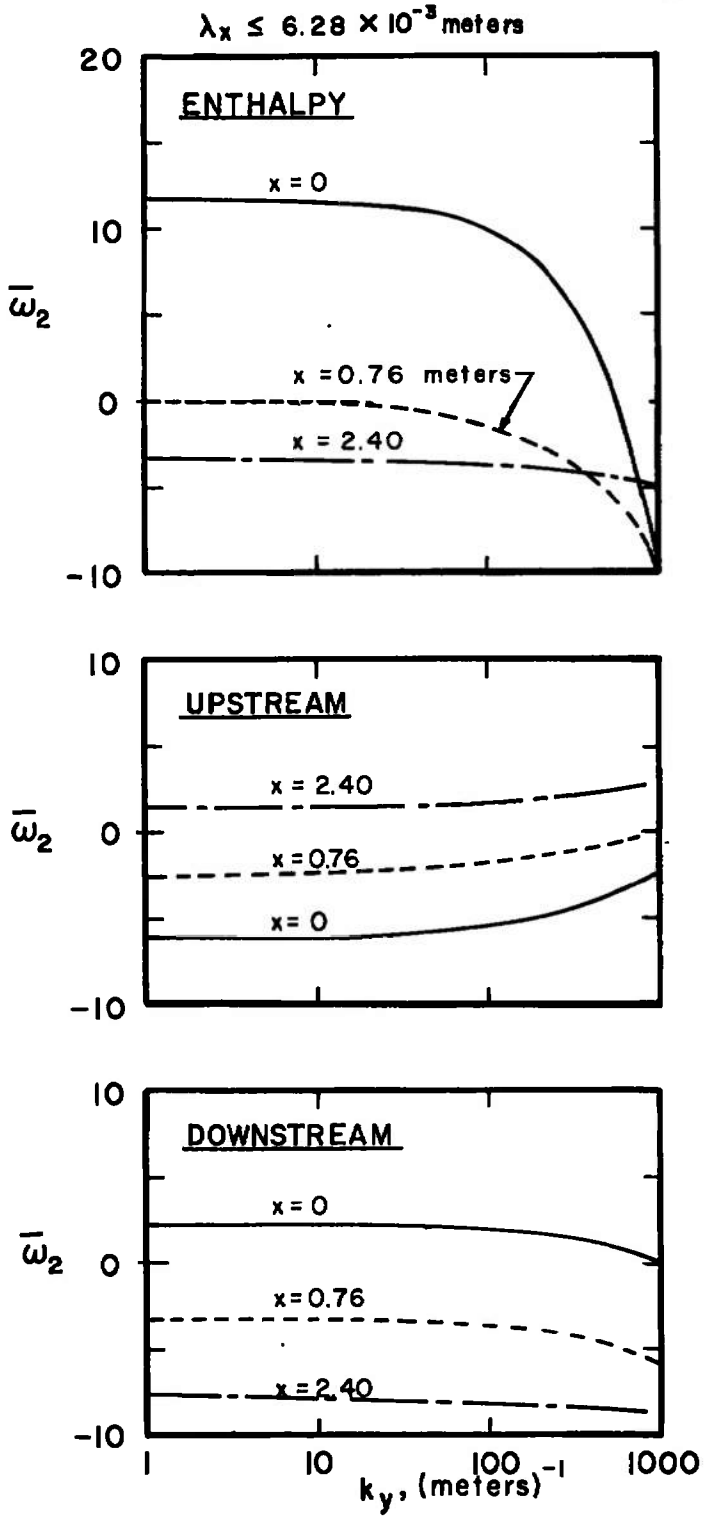

Fig. 16 Growth Rate versus Transverse Wave Number

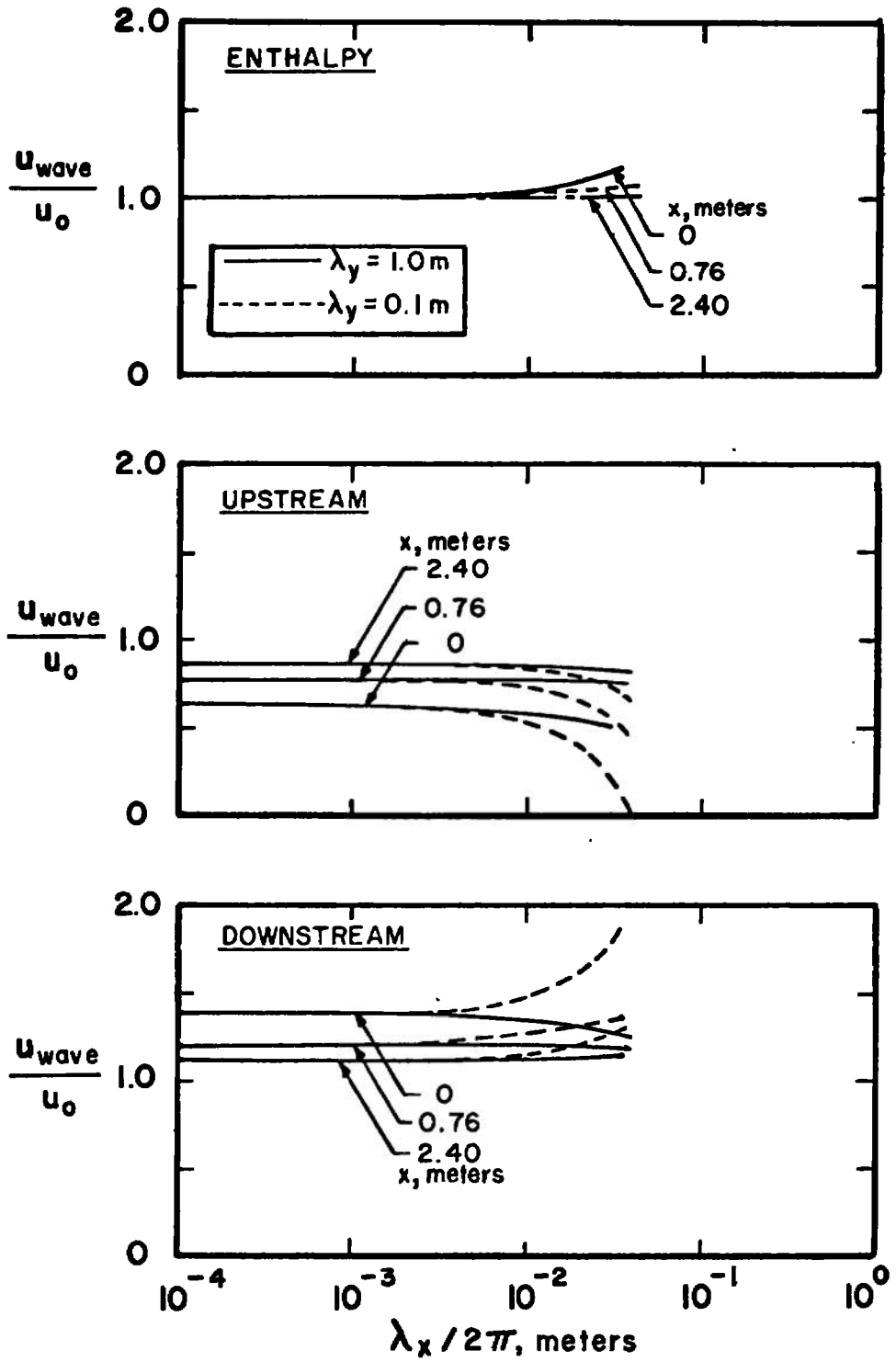

Fig. 17 Wave Speed versus Axial Wavelength

SECTION V
SUMMARY

The linearized stability analyses indicate that axially moving magneto-acoustic and enthalpy waves can be amplified in slant-wall accelerators. The stability and degree of amplification of any wave depend on the electrical boundary conditions and wave form utilized. The imaginary component of the complex frequency ($\bar{\omega}_2$, which indicates the "degree" of instability) was found to be a strong function of the x coordinate. The strong x-dependence was seen to be related to the orientation of the wave with respect to the current vector. The marked x dependence of $\bar{\omega}_2$ and the magnitude of the gradients of ρ_o, u_o, p_o indicate that the analyses are restricted to wavelengths of 0.1 m or less. The disturbance traveled at the local sound speed (relative to the flow) or at the local fluid velocity for short wavelengths, but lost this character as the wavelength increased. In some cases (at wavelengths greater than 0.1 m) the upstream wave moved at a velocity greater than the fluid velocity, and thus would appear to have a negative velocity relative to a fixed observer. However, the validity of the analyses is doubtful at the longer wavelengths.

Table I (Appendix II) summarizes the results of the linearized analyses. The quantity $e^{\omega_2 \overline{T}}$ corresponds to the growth of a disturbance in the device one meter in length with $\bar{\omega}_2$ assumed constant. This only provides an indication of the possible growth of a disturbance since nonlinear effects will become important when the disturbance becomes large. It is predicted, from both the one-dimensional and the two-dimensional analyses, that the enthalpy wave will have the largest growth.

The enthalpy wave is more prone to becoming unstable in a large device ($e_y = j_x = 0$ or 2-D analyses) where the boundaries have no influence on the disturbance. The disturbance oriented at the most favorable angle for amplification would grow. This is not unlike the growth of ionization waves with the resulting striations. The upstream acoustic wave, on the other hand, is more apt to be amplified in small devices where the boundaries have a marked effect on the disturbance ($e_y = \Phi_o e_x$ and $j_x = -\Phi_o j_y$). In this case, the upstream wave is amplified regardless of orientation.

The linearized anlaysis indicates that instabilities can exist in MHD accelerators, but the analysis cannot predict the effect on device performance. A linearized analysis cannot consider the long wavelengths

and aperiodic waves which may be present in MHD devices (Refs. 16 and 17). A more complete analysis which considers the perturbed differential equations subject to the proper boundary conditions is necessary to predict the effect of disturbance growth on accelerator performance.

REFERENCES

1. Kerrebrock, J. L. "Nonequilibrium Ionization Due to Electron Heating." AIAA Journal, Vol. 2, No. 6, p. 1072, June 1964.
2. Evers, W. H. "Wave Phenomena in a Current Carrying Gas." M. S. Thesis, Massachusetts Institute of Technology, September 1966.
3. McCune, J. E. "Wave Growth and Instability in a Partially-Ionized Gas." MHD Electrical Power Generation International Symposium, Paris, July 1964.
4. Velikhov, E. P. "Hall Instability of Current-Carrying Slightly-Ionized Plasmas." MPD Electrical Power Generation Symposium, Kings College, U. of Durham, Newcastle upon Tyne, September 1962.
5. Sutton, G. W. and Witalis, E. A. "Linearized Analysis of MHD Generator Flow Stability." MHD Electrical Power Generation Symposium, Paris, July 1964.
6. Wright, J. K. "A Temperature Instability in Magnetohydrodynamic Flow." Proc. Phys. Soc., Vol. 81, 1963, p. 498.
7. McCune, J. E. "Linear Theory of an MHD Oscillator." Advanced Energy Conversion, Vol. 5, 1965, p. 221.
8. Locke, E. V. and McCune, J. E. "Growth Rates for Axial Magneto-Acoustic Waves in a Hall Generator." AIAA Journal, Vol. 4, October 1966, p. 1748.
9. Briketts, Brian W. "Instability of Magneto-Acoustic Waves in Low-Pressure Plasmas." AIAA Journal, Vol. 6, January 1968, p. 153.
10. Messerle, H. K. "Traveling Wave Interaction and Wave Growth." Sixth Symposium on Engineering Aspects of Magnetohydrodynamics, 1965, p. 104.
11. Sutton, G. W. and Sherman, A. Engineering Magnetohydrodynamics, McGraw-Hill, 1965.

12. de Montardy, A. "An MPD Generator with Series-Connected Electrodes." MPD Electrical Power Generation Symposium, Kings College, U. of Durham, Newcastle upon Tyne, September 1962.

13. Powers, W. L. "Electrical Characteristics and Transient Wave Growth in Magnetogasdynamic Channel." Ph. D. Dissertation, The University of Tennessee, 1967.

14. Landau, L. D. and Lifshitz, E. M. Fluid Mechanics, Addison-Wesley Publishing Company, 1962, p. 313.

15. Morse, D. L. "Low Frequency Instability of Partially-Ionized Plasmas." Physics of Fluids, Vol. 8, 1965, p. 1339.

16. Colgate, S. A. Magnetohydrodynamics, Edited by R. K. M. Landshoff, Stanford University Press, Stanford, California, 1957, p. 104.

17. Fishman, F. J. "Instability of Hall MHD Generators to Magneto-Acoustic Waves." AIAA Journal, Vol. 8, April 1970, p. 632.

APPENDIX I
CURRENT AND JOULE HEATING PERTURBATIONS

In order to relate the perturbed transport quantities (β_1 and σ_1) to the perturbed thermodynamic properties, it is necessary to use the perturbed electron energy equation (Eq. (35))

$$\frac{2\,J_y j_y + 2\,J_x j_x}{J_x^2 + J_y^2} = \left(2\mu_1 + \frac{T_{e_o}}{T_{e_o} - T_o}\right)\frac{T_{e_1}}{T_{e_o}} - \frac{T_o}{T_{e_o} - T_o}\frac{p_1}{p_o} + \left(\frac{2\,S_{m_o}}{2\,S_{m_o} - \alpha_o} + \frac{T_o}{T_{e_o} - T_o}\right)\frac{\rho_1}{\rho_o} \tag{I-1}$$

The perturbed Hall coefficient and electrical conductivity are related to ρ_1, p_1, and T_{e_1} by the following expressions

$$\frac{\sigma_1}{\sigma_o} = a\,\frac{\rho_1}{\rho_o} - \frac{1}{2}\frac{p_1}{p_o} + \left(b + \frac{B_i}{T_{e_o}}\right)\frac{T_{e_1}}{T_{e_o}} \tag{I-2}$$

$$\frac{\beta_1}{\beta_o} = -\frac{1}{2}\frac{p_1}{p_o} + \left(a - \frac{S_{m_o}}{2\,S_{m_o} - \alpha_o}\right)\frac{\rho_1}{\rho_o} + \left\{b + \frac{B_i}{T_{e_o}} - \left(\frac{S_{m_o} - \alpha_o}{2\,S_{m_o} - \alpha_o}\right)\left(\frac{3}{2} + \frac{eV_i}{kT_{e_o}}\right)\right\}\frac{T_{e_1}}{T_{e_o}} \tag{I-3}$$

Using Eqs. (I-1), (I-2), and (I-3), an explicit expression for T_{e_1}/T_{e_o} can be obtained

$$\frac{T_{e_1}}{T_{e_o}} = \varphi_2\frac{u_1}{u_o} + \varphi_3\frac{\rho_1}{\rho_o} + \varphi_4\frac{p_1}{p_o} \tag{I-4}$$

where

$$\varphi_1 = -\left\{ \frac{T_{e_o}}{T_{e_o} - T_o} + \mu_1(2 + q_1 q_4) - q_1(q_3 + q_4)\left(b + \frac{B_i}{T_{e_o}}\right) \right\}$$

$$\varphi_2 = q_1 q_2 / \varphi_1$$

$$\varphi_3 = \frac{1}{\varphi_1}\left\{ \frac{T_o}{T_{e_o} - T_o} + \frac{S_{m_o}}{2S_{m_o} - \alpha_o}(2 + q_1 q_4) - a q_1(q_3 + q_4) \right\}$$

$$\varphi_4 = -\frac{1}{\varphi_1}\left\{ \frac{T_o}{T_{e_o} - T_o} - \frac{q_1}{2}(q_3 + q_4) \right\}$$

$$q_1 = \frac{2 J_y}{J_x^2 + J_y^2} \; ; \; q_2 = \sigma_o u_o B; \quad q_3 = J_y - \beta_o J_x; \quad q_4 = \beta_o J_x$$

Having determined the temperature perturbation, the expressions for the conductivity and Hall coefficient can now be written as

$$\frac{\sigma_1}{\sigma_o} = \xi_1 \frac{p_1}{p_o} + \xi_2 \frac{\rho_1}{\rho_o} + \xi_3 \frac{u_1}{u_o} \tag{I-5}$$

$$\frac{\beta_1}{\beta_o} = \mu_2 \frac{p_1}{p_o} + \mu_3 \frac{\rho_1}{\rho_o} + \mu_4 \frac{u_1}{u_o} \tag{I-6}$$

where

$$\xi_1 = -\frac{1}{2} + \varphi_4\left(b + \frac{B_i}{T_{e_o}}\right)$$

$$\xi_2 = a + \varphi_3\left(b + \frac{B_i}{T_{e_o}}\right)$$

$$\xi_3 = \varphi_2\left(b + \frac{B_i}{T_{e_o}}\right)$$

$$\mu_2 = \xi_1 - \mu_1\varphi_4$$

$$\mu_3 = \xi_2 - \mu_1\varphi_3 - S_{m_o}/(2\,S_{m_o} - \alpha_o)$$

$$\mu_4 = \xi_3 - \mu_1\varphi_4$$

Substituting Eqs. (I-5) and (I-6) into Eqs. (45) and (46) gives the following expressions for the current and joule heating:

$$j_y = a_1\frac{\rho_1}{\rho_o} + a_2\frac{p_1}{p_o} + a_3\frac{u_1}{u_o} \qquad \text{(I-7)}$$

$$E_y j_y + J_x e_x = b_1\frac{\rho_1}{\rho_o} + b_2\frac{u_1}{u_o} + b_3\frac{p_1}{p_o} \qquad \text{(I-8)}$$

where

$$b_1 = \gamma_1\xi_2 + \gamma_2\mu_3$$

$$b_2 = \gamma_3 + \gamma_1\xi_3 + \gamma_2\mu_4$$

$$b_3 = \gamma_1\xi_1 + \gamma_2\mu_2$$

$$a_1 = \xi_2 q_3 + \mu_3 q_4$$

$$a_2 = \xi_1 q_3 + \mu_2 q_4$$

$$a_3 = -q_2 + \xi_3 q_3 + \mu_4 q_4$$

APPENDIX II
TABLE I
SUMMARY OF RESULTS

Analysis	x, m	Enthalpy	Upstream	Downstream
One-Dimensional Perturbation Case I $e_y = j_x = 0$	0.0	Amplified $e^{\omega_2 \bar{T}} \approx 10^5$	Attenuated	Neutral $\omega_2 \approx 0$
	0.76	Neutral $\omega_2 \approx 0$	Attenuated	Attenuated
	2.4	Attenuated	Amplified $e^{\omega_2 \bar{T}} \approx 25.0$	Attenuated
One-Dimensional Perturbation Case II $e_y = \Phi_o e_x$ $j_x = -\Phi_o j_y$	0.0	Attenuated	Amplified $e^{\omega_2 \bar{T}} \approx 40$	Attenuated
	0.76	Attenuated	Amplified $e^{\omega_2 \bar{T}} \approx 300$	Attenuated
	2.4	Attenuated	Amplified $e^{\omega_2 \bar{T}} \approx 300$	Attenuated
Two-Dimensional Perturbation $\lambda_y = 1$ m	0.0	Amplified $e^{\omega_2 \bar{T}} \approx 10^5$	Attenuated	Amplified $e^{\omega_2 \bar{T}} \approx 4.4$
	0.76	Amplified $\omega_2 \approx 0.016$	Attenuated	Attenuated
	2.4	Attenuated	Amplified $e^{\omega_2 \bar{T}} \approx 7$	Attenuated

$\bar{T}$ - Time spent in device one meter in length

UNCLASSIFIED

Security Classification

DOCUMENT CONTROL DATA - R & D

(Security classification of title, body of abstract and indexing annotation must be entered when the overall report is classified)

1. ORIGINATING ACTIVITY *(Corporate author)*
Arnold Engineering Development Center
ARO, Inc., Operating Contractor
Arnold Air Force Station, Tennessee 37389

2a. REPORT SECURITY CLASSIFICATION
UNCLASSIFIED

2b. GROUP
N/A

3. REPORT TITLE
INSTABILITIES IN MHD ACCELERATORS

4. DESCRIPTIVE NOTES *(Type of report and inclusive dates)*
Final Report, July 1967 to July 1968

5. AUTHOR(S) *(First name, middle initial, last name)*
G. W. Garrison, ARO, Inc.

6. REPORT DATE	7a. TOTAL NO. OF PAGES	7b. NO. OF REFS
February 1971	63	17

8a. CONTRACT OR GRANT NO.	9a. ORIGINATOR'S REPORT NUMBER(S)
F40600-71-C-0002	
b. PROJECT NO.	AEDC-TR-70-290
c. Program Element 64719F	9b. OTHER REPORT NO(S) *(Any other numbers that may be assigned this report)*
d.	ARO-PWT-TR-70-265

10. DISTRIBUTION STATEMENT
This document has been approved for public release and sale; its distribution is unlimited.

11. SUPPLEMENTARY NOTES	12. SPONSORING MILITARY ACTIVITY
Available in DDC.	Arnold Engineering Development Center, AFSC, Arnold Air Force Station, Tennessee 37389

13. ABSTRACT

A linearized perturbation analysis is used to determine if instabilities can occur in MHD accelerators. When the electrical perturbations are assumed unaffected by the presence of conducting walls, the enthalpy wave has the largest growth rate. The growth rate depends upon the orientation of the current vector to the wave front and the location within the accelerator. When the electrical perturbations are influenced by the presence of the slanted conducting walls, the upstream-moving magneto-acoustic wave is amplified. When steady-state gradients are neglected, the growth rate changes only slightly in both cases. An elevated electron temperature increases the enthalpy wave growth rate in the absence of conducting walls, but has little effect when the conducting walls control the electrical perturbations. The linearized analysis indicates that instabilities can exist in MHD accelerators and the growth rate may be large in some cases.

DD FORM 1 NOV 68 1473

UNCLASSIFIED

Security Classification

14. KEY WORDS	LINK A		LINK B		LINK C	
	ROLE	WT	ROLE	WT	ROLE	WT
magnetohydrodynamics						
plasma accelerations						
linear accelerators						
magnetic fields						
stability						
perturbation						
wave functions						
enthalpy						